Gaussian Two-Way Channel with Constellation-based Input

by

Seyedershad Banijamali

A thesis
presented to the University of Waterloo
in fulfillment of the
thesis requirement for the degree of
Master of Applied Science
in
Electrical and Computer Engineering

Waterloo, Ontario, Canada, 2013

I hereby declare that I am the sole author of this thesis. This is a true copy of the thesis, including any required final revisions, as accepted by my examiners.

I understand that my thesis may be made electronically available to the public.

Abstract

Achieving a higher transmission rate had always been a goal in the field of communications. Having a two-way channel in which two nodes transmit and receive data at the same time, is an important tool to achieve this goal. A two-way channel is the first step from point-to-point communication channel toward multi-user networks. In its ideal form, we can transmit data two times faster by using a perfect two-way channel. However, the area of two-way channels had not been of interest of researchers during the past years and number of articles on this area is considerably low comparing to other types of multi-user communication networks, such as multiple-access channel, broadcast channel and interference channel.

On the other hand, use of analog-to-digital converters (ADC) is a must in modern systems to enable us to analyze data faster; nevertheless, presence of ADC add some other difficulties to the system.

In this thesis, different scenarios about two-way channel are studied. The Shannon's model of two-way channel and his inner and outer bounds on the capacity of this channel are presented. For the Gaussian Two-Way Channel with quantized output, in which the ambient noise has a Gaussian distribution, the expression of Shannon's inner bound for both Gaussian and discrete inputs are derived.

The best uniform quantizer to obtain the maximum achievable rate for Gaussian input is found numerically. Then we will evaluate the additive noise model for the quantizer from an information theoretic point of view.

For the discrete input, the method of rotating one input with respect to other one is employed to enlarge the achievable rate region.

At last, two scenarios will be studied in which, minimizing the power of interference, does not necessarily maximizes the transmission rate.

Acknowledgements

An special thanks to my great supervisor, Prof. Amir Khandani. And I also would like to thank Dr. K. Moshksar.

Dedication

This is dedicated to my dear Parents and my love, Mina.

Table of Contents

List of Tables

List of Figures

Chapter 1

Introduction

In this chapter we will study a variety of subjects related to our works. We will have a glance on prior arts and what has been done by researchers so far.

First of all, in the next section, basics of Two-way Channel, which is the main topic of this thesis, is presented. A short history of this channel is given and different features will be investigated.

In the next section, a study on quantization is presented. We will see how we can model a quantizer in our systems and it affects the performance. Quantization noise is then looked at and best model of its pdf will be introduced.

In section 3, we will see a scenario which is called erasure channel for a point to point communication. This type of channel has been also studied in this thesis for Two-Way channel.

But, we need first to know what has been done on this topic before. So, a short discussion on very important paper on this topic will be given.

1.1 Two-Way Channel: A short review

Two-way channel, for the first time, has been introduced by Shannon [1] in 1961. In that paper Shannon described properties of a two- way channel in general. A two-way channel consists of two users, trying to send information to each other through a common path. A simple model of two-way channel has been depicted in Fig. 1.1.

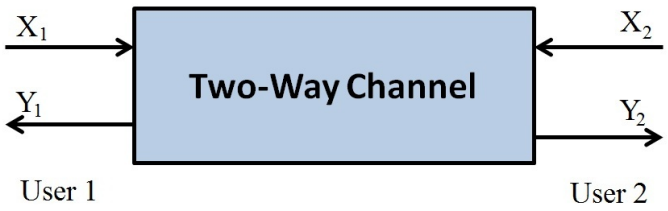

Figure 1.1: A simple model of Two-way Channel

To study a two-way channel we will enter the field of network information theory. The capacity of a two-way channel in its general form is still an open problem. But, in [1], Shannon derived both an inner bound and an outer bound for the capacity region of a two-way channel. These two bounds, coincide in some cases of two-way channel. But, in most cases there is a gap between Shannon's proposed bounds. For example, for MOD 2 adder (Fig 1.2) as a Two-way channel introduced in Shannon's paper, these two bounds coincide.

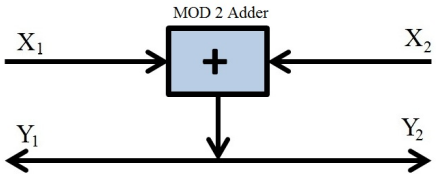

Figure 1.2: An Example of Two-way channel in which Shannon's bounds coincide

But, for Binary Multiplying Channel (BMC) (Fig. 1.3), where the adder is substituted with an AND gate, these bounds do not coincide.

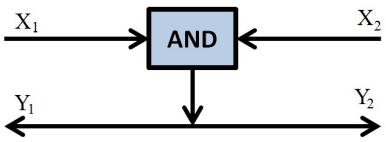

Figure 1.3: An Example of Two-way channel in which Shannon's bounds do not coincide

For the BMC channel shown in the above figure, Schalkwijk in [2] proposed a new coding scheme that leads to a achievable rate beyond Shannon's inner bound. He also improved this achievable rate later in [3] and [4]. In 1995, an even better scheme introduced for this particular channel in [5].

Each node at two-way channel has both transmitter and receiver antennas. These two antennas are close to each other. A very common phenomenon in two-way channel is self-interference or leakage signal, which is the signal from transmitter to receiver of one node.

In 1984, for the general case of two-way channel, Han derived a higher achievable rate than Shannon's inner bound in [6]. In this paper, he also calculated the exact capacity of Gaussian Two-Way (GTW) channel, and showed that for this scenario, the two-way channel can be modelled as two parallel channels with Gaussian noise and the capacity region is rectangular.

A new outer bound on the capacity of two-way channel has been introduced in [7]. In this work the bound is derived by introducing two auxiliary random variables.

After these works the area of capacity of two-way channel has not been investigated so much.

Throughout this thesis we will consider two independent codebooks for users and try to enlarge Shannon's achievable rate region.

1.2 Quantization in Communication

Another topic that will play an important role in this thesis is *Quantization*. In the modern communication systems, quantization is an inevitable part. Most of signal processing at the receiver side are performed after an analog-to-digital conversion and quantization is a part of this conversion.

Our model of two-way channel is also Gaussian, with uniform quantizers at receivers. Use of quantizer at receivers has been studied recently in some works. In [8] and [9], it has been shown that for point-to-point channel, when we quantize the output of the channel, the capacity achieving input distribution has to be discrete. In fact it has been proven that use of quantizer imposes an additional peak-power constraint on the input random variable and according to [10] the input has to be discrete. In [11] and [12] the author considered output quantization for MAC and Broadcast channel with discrete input.

Different aspects of quantization has been studied so far. In this thesis, the main feature that we will face through using a quantizer is *Quantization error* or *Quantization noise*. We will consider an additive model for this error. So it is defined as the difference between the value of the quantizer's input signal and the value of the quantizer's output. This quantization noise is well-studied at [13] and [14].

We will use both Gaussian and discrete random variables as the channel input.

1.3 Gaussian Erasure Channel

In the third chapter of this thesis we will consider a Gaussian Erasure two-way channel. In this channel the messages can be completely erased with some probability distribution of erasure, and receiver only receives the channel noise. In [15] the capacity of Gaussian Erasure point-to-point channel is studied and the asymptotic expressions for the capacity is found.

Chapter 2

Two-Way Channel with Output Quantization

2.1 Introduction and Preliminaries

In this chapter we will discuss about basics of two-way channel and the model which introduced by Shannon in 1961. Then Gaussian Two-Way (GTW) channel and Han's argument ([6])about this particular, but important, type of two-way channel will be presented. Then we will discuss about our own model in which, a quantizer is added at both receiver ends.

2.1.1 Shannon's Model of Two-way channel and Prior Arts

Shannon proposed a discrete memoryless two-way channel. His model of two-way channel has been shown in Fig. 2.1 [1].

In this figure, f and g are encoding functions and φ and ψ are decoding functions. m_1 and m_2 are input messages for user1 and user2 respectively. m_1 is chosen from set $\mathcal{M}_1 = \{1, 2, ..., M_1\}$ and m_2 is chosen from set $\mathcal{M}_2 = \{1, 2, ..., M_2\}$. $P(y_1, y_2|x_1, x_2)$ is the channel transition probability function. X_1 and X_2 are channel inputs and Y_1 and Y_2

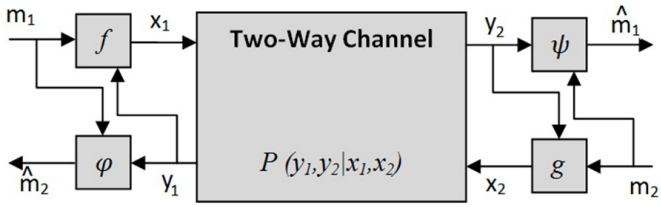

Figure 2.1: Shannon's model of Two-Way channel

are channel output alphabet sets. For encoding a message, each user, uses both current message and a sequence of received symbols from the other user. Similarly, decoding at each receiver end depends on the message sent and the sequence of received symbols. For a block code of length n, the encoding functions are as follow:

$$\begin{aligned} x_1^n &= (f_0(m_1), f_1(m_1, y_{11}), f_2(m_1, y_{11}, y_{12}), ..., f_{n-1}(m_1, y_{11}, ..., y_{1,n-1})) \\ x_2^n &= (g_0(m_2), g_1(m_2, y_{21}), g_2(m_2, y_{21}, y_{22}), ..., g_{n-1}(m_2, y_{21}, ..., y_{2,n-1})) \end{aligned} \tag{2.1}$$

The probability of error at each terminal is then defined as the following:

$$\begin{aligned} P_{e_1} &= \tfrac{1}{M_1 M_2} \sum_{m_1=1}^{M_1} \sum_{m_2=1}^{M_2} P(m_1 \neq \hat{m}_1 | m_1, m_2 \text{were sent}) \\ P_{e_2} &= \tfrac{1}{M_1 M_2} \sum_{m_1=1}^{M_1} \sum_{m_2=1}^{M_2} P(m_2 \neq \hat{m}_2 | m_1, m_2 \text{were sent}) \end{aligned} \tag{2.2}$$

Let us denote the rate of the code-book that carries information from transmitter 1 to receiver 2 by R_1 and from transmitter 2 to receiver 1 by R_2.

Now, pair (R_1, R_2) is an achievable pair rate if for $\eta > 0$ and any $0 < \lambda < 1$ there exists a code (n, M_1, M_2) such that:

$$\begin{aligned} (\tfrac{1}{n}) \log M_1 &\geq R_1 - \eta \\ (\tfrac{1}{n}) \log M_2 &\geq R_2 - \eta \end{aligned} \tag{2.3}$$

and

$$\begin{aligned} P_{e_1} &\leq \lambda \\ P_{e_2} &\leq \lambda \end{aligned} \tag{2.4}$$

The set of all achievable pair rates form the capacity region of two-way channel [6].

Shannon bounds on the capacity of Two-Way channel

The capacity region of a two-way channel in its general form is still unknown. In [1], Shannon established inner and outer bounds on the capacity region of a two-way channel. The outer bound includes all pairs of (R_1, R_2) satisfying the inequalities

$$\begin{aligned} R_1 &\leq I(X_1; Y_2|X_2) \\ & \quad , \\ R_2 &\leq I(X_2; Y_1|X_1) \end{aligned} \tag{2.5}$$

where X_1 and X_2 have an arbitrary joint distribution $p(x_1, x_2)$. As for inner bound, these expressions still hold, however, X_1 and X_2 are independent random variables $p(x_1, x_2) = p(x_1)p(x_2)$.

In this thesis we will try to enlarge this achievable rate region introduced by Shannon for different scenarios.

New inner bound

For this model, Han in [6] introduced a new achievable rate region. According to his work the new achievable rates can be found by defining a new random variable and block Markov coding strategy. This new achievable rate region completely includes Shannn's proposed inner bound and so it is a new inner bound for two-way channel. The cardinality of the auxiliary random variable is assumed to be finite and thus the inner bound is computable.

To understand the achievable rate region of Han, a test channel is needed to be introduced. This test channel is depicted in figure 2.2.

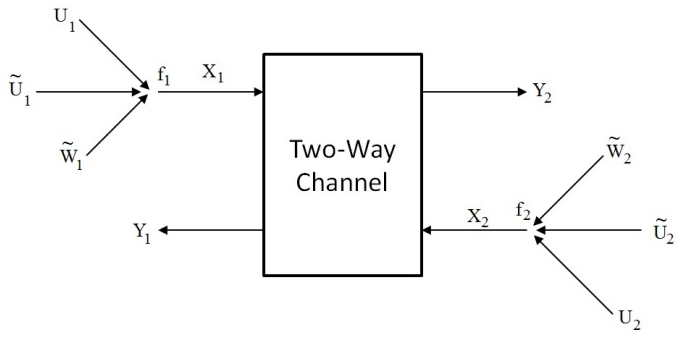

Figure 2.2: Han's test channel

As it is shown in this figure, each channel input X_i is generated using three auxiliary random variables, U_i, $\tilde{U}_i$ and $\tilde{W}_i$. Where U_i carries the new message information, $\tilde{U}_i$ carries previous message information, and $\tilde{W}_i$ carries the feedback information from the output terminals [6]. These three auxiliary random variables then produce channel inputs under f_i's as the encoding functions:

$$\begin{aligned} X_1 &= f_1(U_1, \tilde{U}_1, \tilde{W}_1) \\ X_2 &= f_2(U_2, \tilde{U}_2, \tilde{W}_2) \end{aligned} \tag{2.6}$$

The relation between auxiliary random variables is defined as the following (for $i = 1, 2$):

$$\begin{aligned} \tilde{U}_i^t &= U_i^{(t-1)} \\ \tilde{W}_i &= X_i^{(t-1)} Y_i^{(t-1)} \end{aligned} \tag{2.7}$$

Han's encoding scheme is different from Shannon's scheme in [1]. Shannon updates the channel input signal bit by bit using the current message and the received feedback. But here, Han's scheme uses a completely similar encoding scheme stated in [23]. Actually a block Markov technique.

The main theorem of Han is the following:

Theorem 2.1.1. *(Han [6]) If we define these inequalities:*

$$\begin{aligned} R_1 &\leq I(\tilde{U}_1; X_2 Y_2 \tilde{U}_2 \tilde{W}_2) \\ R_2 &\leq I(\tilde{U}_2; X_1 Y_1 \tilde{U}_1 \tilde{W}_1) \end{aligned} \tag{2.8}$$

and set $\mathcal{R}$ as below:

$$\mathcal{R} = \bigcup (R_1, R_2) \tag{2.9}$$

Then every element of $\mathcal{R}$ is achievable.

New outer bound

After Han's work, in 1986, a new outer bound to the capacity of two-way channel derived in [7]. This new outer bound also derived by using auxiliary random variables. The main theorem of this paper is the following:

Theorem 2.1.2. *(Zhang [7]) The capacity region $\mathcal{R}$ of a two-way channel is a subset of the region*

$$\begin{aligned} \mathcal{R}^* \equiv \{((R_1, R_2) \quad &: \\ R_1 \quad &\leq min[H(X_1|Z_1), I(X_1; Y_2|X_2, Z_2)] \\ R_1 \quad &\leq min[H(X_2|Z_2), I(X_2; Y_1|X_1, Z_1)] \end{aligned} \tag{2.10}$$

where $X_1, X_2, Y_1, Y_2, Z_1, Z_2$ are random variables whose joint distribution is of the form:

$$p(z_1, z_2)p(x_1|z_1)p(x_2|z_2)p(y_1, y_2|x_1, x_2)$$

and $p(y_1, y_2|x_1, x_2)$ is the channel transition probability.

X_i can be assumed to be generated by Z_i. Z_i itself can be considered as the combination of the past message information and the feedback of the terminal i. Therefore, the amount of new information in X_i is actually $H(X_i|Z_i)$. $I(X_i; Y_j|X_j, Z_j)$ (and $i \neq j$) is an upper

bound that is imposed by two-way channel itself. Consequently, the forward direction rate is less than the minimum of these two values.

2.1.2 Gaussian Two-Way Channel (GTWC)

A Gaussian Two-Way Channel (GTWC) has been shown in figure 2.3.

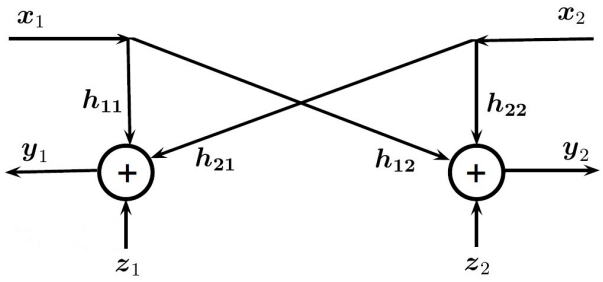

Figure 2.3: Gaussian Two-Way channel, Z_1 and Z_2 are Gaussian random variables

According to this figure we have:

$$\begin{aligned} Y_1 &= h_{11}X_1 + h_{21}X_2 + Z_1 \\ &\quad , \\ Y_2 &= h_{12}X_1 + h_{22}X_2 + Z_2 \end{aligned} \tag{2.11}$$

where X_1 and X_2 represent the transmitted signals and Z_1 and Z_2 are additive noises at the receiver sides. Moreover, Z_1 and Z_2 are Gaussian independent random variables. For each terminal the signal from transmitter to its own receiver is not desired and acts as an interference signal. Because this signal goes from transmitter to receiver of one node we call it *Self-Interference*. Due to the nature of this system, the interfering signal has much higher power than the desired signal, i.e., h_{11} and h_{22} are much larger than h_{12} and h_{21}, respectively. Using RF techniques, one may considerably reduce self-interference [22]. Because this signal is known for the receiver, the receiver tries to cancel it. In a scenario where we impose a power constraint over input signals, Han in [6], derived the

exact expression for the capacity region of GTWC. He presented this result in the following theorem

Theorem 2.1.3. *[6] The capacity region of GTWC with power constraint P_1 and P_2 is the set of all (R_1, R_2) such that*

$$\begin{aligned} R_1 &\leq \tfrac{1}{2}\log\left(1+\tfrac{{h_{12}}^2 P_1}{\sigma_z^2}\right) \\ R_2 &\leq \tfrac{1}{2}\log\left(1+\tfrac{{h_{21}}^2 P_2}{\sigma_z^2}\right) \end{aligned} \quad . \tag{2.12}$$

It is seen that the capacity achieving inputs are Gaussian and each side can completely cancel the self-interference. As such, GTWC is equivalent to two orthogonal (parallel) Gaussian point-to-point channels.

2.1.3 Gaussian Two-Way Channel with output Quantization

Quantization is an inevitable part of modern communication systems. Most of signal processing operations at the receiver side are performed after the analog-to-digital conversion stage. In the rest of this chapter, we address a GTWC with quantized outputs. The system model is shown in figure 2.4

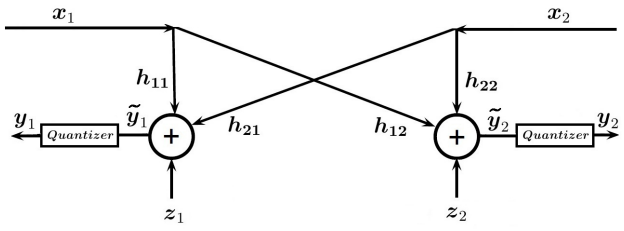

Figure 2.4: Model of Two-Way channel with output quantization

Using this figure we have the following:

$$\begin{aligned} Y_1 &= \mathcal{Q}(\tilde{Y}_1) = \mathcal{Q}(h_{11}X_1 + h_{21}X_2 + Z_1) \\ Y_2 &= \mathcal{Q}(\tilde{Y}_2) = \mathcal{Q}(h_{12}X_1 + h_{22}X_2 + Z_2) \end{aligned}, \tag{2.13}$$

where Y_1 and Y_2 are the quantized outputs and $\mathcal{Q}(\cdot)$ is quantization function. Since quantization is not a linear operation, users cannot cancel the effect of self-interference anymore. Therefore, in contrast to GTWC, Gaussian inputs are not necessarily optimal.

We utilize identical quantizers with a finite number of quantization levels at both ends. The step size of the quantizers is denoted by q. The output of the quantizer can assume any of the M real numbers in the set $\mathcal{Y} = \{l_1, l_2, ..., l_M\}$. In fact, $\mathcal{Q}(y) = l_i$ whenever $y \in \mathcal{R}_i = [b_{i-1}, b_i]$ where

$$\begin{aligned} b_0 &= -\infty \\ b_M &= +\infty \\ b_i &= \left(i - \tfrac{M}{2}\right) q, \quad i \in \{1, 2, ..., M-1\}. \end{aligned} \tag{2.14}$$

We take SNR $\triangleq \frac{P}{\sigma_z^2}$ as a measure of SNR. In [8, 9], it is shown that in a point-to-point Gaussian channel with quantized output, the capacity achieving input distribution is discrete with a finite number of mass points. In the setup of a GTWC with quantized outputs, our results confirm the supremacy of discrete inputs over Gaussian inputs at least in the low SNR regime. As such, the majority of this chapter is devoted to constellation-based transmitters.

In [8] it is proposed that the loss in mutual information between the input and output of a point-to-point channel due to low-precision quantization is tolerable and even for high values of SNR (20 dB), 3-bit quantizers do not decrease the performance more than 15% compared to infinite precision quantization. Motivated by this observation, we rely on 8-level (3-bit) quantizers in our simulations unless otherwise stated.

The rest of this chapter is organized as follow. In section 2.2, performance of Gaussian

inputs is studied and optimum step size of quantizer is computed numerically for some SNRs. In section 2.3, for 1-dimensional and 2-dimensional scenarios the expression for channel capacity with constellation-based inputs is derived. Then, we consider a θ degrees rotation in constellation of one of the users, and investigate its effects on capacity region.

2.2 Gaussian Inputs

Although Gaussian inputs are not necessarily optimal for our problem, it is still of interest to evaluate their performance in this model.

2.2.1 Why Gaussian?

Achieving a high rate data transmission is a goal in modern communication systems, specially in mobile devices. An important obstacle that these systems experience is multipath fading. To overcome this problem, a common way is to employ multi-carrier signals, such as OFDM [25]. The main advantages of OFDM signal are: robustness against fading caused by multipath propagation and against Inter-Symbol Interference, robustness against narrow-band co-channel interference, easily adaption to severe channel conditions without complex equalization, and simple implementation using Fast-Fourier Transform(FFT). But, an important problem of OFDM signals is their high Peak to Average Power Ratio (PAPR), specially when number of carriers is large.

On the other hand, as we stated above, use of analog-to-digital converter is a must in modern systems. This means that the received signal first goes through a quantizer.

In this section, we utilize the OFDM signals as the input of a two-way channel.

We suppose the channel inputs are chosen from constellations with N points $\mathcal{S}_1$ and $\mathcal{S}_2$.

$$\begin{matrix} \mathcal{S}_1 = \{s_{11}, s_{12}, ..., s_{1N}\} \\ \\ \mathcal{S}_1 = \{s_{21}, s_{22}, ..., s_{2N}\} \end{matrix} , \tag{2.15}$$

s_{ij}'s are complex numbers. These points are then transmitted over the channel under OFDM modulation. We denote the modulated signal by $S_i(t)$, for $i \in \{1, 2\}$:

$$S_i(t) = \sum_{k=1}^{N} s_{ik} e^{-j\omega_k t}. \tag{2.16}$$

where:

$$S_i(t) = X_i(t) + jY_i(t) \tag{2.17}$$

In [16], it has been rigorously proven that bandlimited OFDM signal converges to a stationary complex Gaussian random process when number of sub-carriers goes to infinity, i.e. both real and imaginary part of the signal will converge to a Gaussian random process. For the sake of simplicity, we just study the real part of the signal. The results can be extended to the imaginary part as well. We suppose N is large enough such that we can substitute $X_i(t)$ by X_i which is a Gaussian random variable.

Because we would like to study the achievable rate region introduced by Shannon [1] we consider two independent Gaussian signals as the channel inputs. We also assume that $h_{11} = h_{22}$ and $h_{12} = h_{21}$. Moreover, we impose the same power constraint over inputs, i.e. $P_1 = P_2 = P$. In this condition $\tilde{Y}_1$ and $\tilde{Y}_2$ in figure 2.4 are Gaussian random variables with the following pdf's.

$$f_{\tilde{Y}_1}(\tilde{y}_1) = \frac{1}{\sqrt{2\pi((h_{11}{}^2 + h_{21}{}^2)P + \sigma_{z_1}{}^2)}} \exp\Big(- \frac{\tilde{y}_1^2}{2((h_{11}{}^2 + h_{21}{}^2)P + \sigma_{z_1}{}^2)}\Big) \tag{2.18}$$

$$f_{\tilde{Y}_2}(\tilde{y}_2) = \frac{1}{\sqrt{2\pi((h_{12}{}^2 + h_{22}{}^2)P + \sigma_{z_2}{}^2)}} \exp\Big(- \frac{\tilde{y}_2^2}{2((h_{12}{}^2 + h_{22}{}^2)P + \sigma_{z_2}{}^2)}\Big) \tag{2.19}$$

Due to symmetry, we focus on computing R_1. According to (2.5), we need to compute $I(X_1; Y_2|X_2)$. Note that Y_2 is a quantized version of $\tilde{Y}_2$ and is a discrete random variable. Deriving a closed form for this conditional mutual information is unlikely. However, we can compute it numerically and find the optimum quantizer.

In the next subsections we consider a uniform finite-level quantizer $\mathcal{Q}$ at both receiver

ends. In subsection 2.2.2 for differnt values of input power (P) we find the optimum step-size of quantizer. In subsection 2.2.3 we will try to find a model for additive quantization noise.

For the rest of this chapter we suppose: $\sigma_{Z_1} = \sigma_{Z_2} = \sigma_Z$.

2.2.2 Optimum step size for Gaussian Input

In this subsection, we will find the best uniform quantization step size for a fixed number of levels (M is fixed) that maximizes the Shannon acheivable rate from terminal 1 to terminal 2. To do so we utilize the expression for conditional mutual information.

$$I(X_1; Y_2|X_2) = H(Y_2|X_2) - H(Y_2|X_1, X_2) \tag{2.20}$$

Fig. 2.5 demonstrates the optimum step size of output quantizers, which maximizes the rate, for different values of SNR.

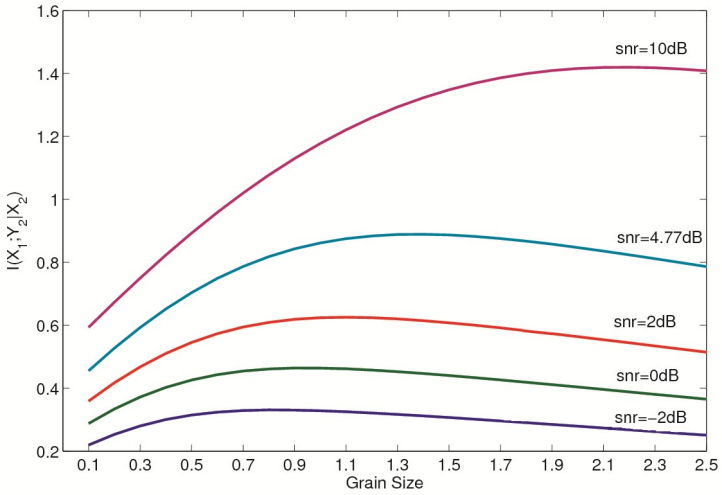

Figure 2.5: Optimum quantizer step size for GTWC with Gaussian inputs at different SNRs

The following observations can be made from this figure:

1- Low-precision quantizing does not affect performance considerably. For example, at SNR = 4.77 dB, the best rate we can achieve is 0.89 bits/sec/hz with step size 1.3. If we do not use a quantizer, this rate would be 1 bits/sec/hz according to (2.12). This implies that there is about 10% loss due to 3-bit quantization in contrast to the case with no quantization.

2- Given number of quantization levels, M, there is only one optimum step size. In fact, for small step sizes, the quantizer cannot cover the whole dynamic range of its input. On the other hand, as we increase the step size, the resolution decreases. This results in loss of information as well. The reduction continues until we reach a point in which almost the whole signal lies in one step and the amount of $I(X_1; Y_2 \mid X_2)$ converges to a certain number (e.g., 0.37814 for SNR = 4.77 dB).

3- As SNR increases the dynamic range of the signal at the quantizer input grows and the optimum step size increases accordingly.

2.2.3 How to model the Quantization noise?

In this subsection we want to replace the quantizer with an additive noise and then see how appropriate is this model by comparing the achievable rates obtained using each model. Let's consider n as the additive quantization noise which is defined as the following:

$$N = X - \mathcal{Q}(X) \tag{2.21}$$

where X is the input signal of the quantizer. In [13] and [14] quantization noise is well studied. In both of these works for an infinite-level quantizer a necessary and sufficient condition for the quantization noise to be white and uniform is expressed. A condition under which the input signal and quantization noise are uncorrelated is also proposed.

It can be easily shown that the pdf of quantization noise is:

$$f_N(n) = \begin{cases} \frac{1}{q} + \frac{1}{q} \sum_{i \neq 0} \Psi_X(\frac{2\pi i}{q}) \exp(-j\frac{2\pi i n}{q}) & q/2 \leq n < q/2 \\ 0 & \text{otherwise.} \end{cases} \tag{2.22}$$

Where $\Psi_X(.)$ is the characteristic function of the random variables X and is defined as below:

$$\Psi_X(u) = E[\exp(jux)] \tag{2.23}$$

Theorem 2.2.1. *(Sripad [14]) The pdf of quantization noise is uniform*

$$f_N(n) = \begin{cases} \frac{1}{q} & q/2 \leq n < q/2 \\ 0 & \textit{otherwise.} \end{cases} \tag{2.24}$$

if and only if the characteristic function of the input random variable has the following property:

$$\Psi_X(\tfrac{2\pi i}{q}) = 0, \textit{ for all } i \neq 0$$

The above theorem explains the necessary and sufficient condition for the quantization noise to be uniform. So N is a uniform random variable with zero mean and variance: $\sigma_N^2 = q^2/12$. The same condition is a sufficient condition for quantization input signal and quantization noise to be uncorrelated [14].

But according to our model, the input signal of the quantizers in the receiver sides are Gaussian (see (2.19)). We also know that the characteristic function and pdf of a random variable are Fourier pair. This issues together with the fact that the Fourier transform of Gaussian signals is also Gaussian, yields that the input signal of our quantizers does not satisfy the condition in the above theorem.

In [13] it is shown that if the quantization step size is fine enough, we can approximately use the results of the above theorems.

Now, we would like to evaluate this approximation from an information theoretic point of view, i.e. we model the quantizer by an additive uniform noise which is *independent*

of quantizer's input signal (however in the above theorem, if the condition is satisfied, quantizer noise and the input signal are assumed to be uncorrelated).

Again we calculate R_1 (transmission rate from user 1 to user 2) and results are extendable to R_2. According to this assumption we have:

$$Y_2 = \mathcal{Q}(\tilde{Y}_2) = h_{12}X_1 + h_{22}X_2 + Z_2 + N_2 \tag{2.25}$$

where N_2 is the additive uniform quantization noise at receiver 2.

Now the expression of achievable rate according to Shannon's inner bound is:

$$\begin{aligned} R_1 \leq I(X_1; Y_2|X_2) &= h(Y_2|X_2) - h(Y_2|X_1, X_2) \\ &\stackrel{a}{=} h(h_{12}X_1 + h_{22}X_2 + Z_2 + N_2|X_2) - h(h_{12}X_1 + h_{22}X_2 + Z_2 + N_2|X_1, X_2) \\ &\stackrel{b}{=} h(h_{12}X_1 + Z_2 + N_2|X_2) - h(Z_2 + N_2|X_1, X_2) \\ &\stackrel{c}{=} h(h_{12}X_1 + Z_2 + N_2) - h(Z_2 + N_2) \end{aligned} \tag{2.26}$$

Where (a) comes from (2.25), (b) comes from properties of differential entropy, and (c) comes from independence of random variables.

In the above expression, $h_{12}X_1 + Z_2 + N_2$ and $Z_2 + N_2$ are both sum of two independent Gaussian and uniform random variables[1]. We know that the pdf of sum of two independent random variable is equal to convolution of their pdf. For a Gaussian random variable $G \sim N(0, {\sigma_g}^2)$ and uniform random variable $U \sim Unif(-q/2, q/2)$ we have:

$$S = G + U$$

So $f_S(s) = (f_G * f_U)(s)$, where f_G is Gaussian pdf and f_U is Uniform pdf.

$$f_S(s) = \int_{-q/2}^{q/2} \frac{1}{q} \frac{1}{\sqrt{2\pi{\sigma_g}^2}} \exp(-\frac{(s-x)^2}{2{\sigma_g}^2}) \mathrm{d}x = \frac{1}{q}\big(\phi(\frac{-q/2 - s}{\sigma_g}) - \phi(\frac{q/2 - s}{\sigma_g})\big) \tag{2.27}$$

[1] In $h_{12}X_1 + Z_2 + N_2$ the Gaussian random variable is $h_{12}X_1 + Z_2$ with variance ${h_{12}}^2 P_1 + {\sigma_Z}^2$.

Now, for the last line of (2.26), suppose the following expressions:

$$\begin{aligned} S_1 &= h_{12}X_1 + Z_2 + N_2 \\ S_2 &= Z_2 + N_2 \end{aligned} \tag{2.28}$$

Then:

$$R_1 \leq I(X_1; Y_2|X_2) = h(S_1) - h_(S_2) \tag{2.29}$$

where pdf of S_1 and S_2 are as below:

$$f_{S_1}(s) = \frac{1}{q}\big(\phi(\frac{-q/2 - s}{\sqrt{{h_{12}}^2 P_1 + {\sigma_Z}^2}}) - \phi(\frac{q/2 - s}{\sqrt{{h_{12}}^2 P_1 + {\sigma_Z}^2}})\big) \tag{2.30}$$

$$f_{S_2}(x) = \frac{1}{q}\big(\phi(\frac{-q/2 - s}{\sigma_Z}) - \phi(\frac{q/2 - s}{\sigma_Z})\big) \tag{2.31}$$

To evaluate the additive noise model for the quantizer we compare the Shannon's achievable rate obtained from (2.29) (additive model) with achievable rate obtained by using quantizer itself. Figures below show this comparison. For these simulations we suppose that the power of channel noise is 1 and the power of signal is 3. Channel gains are identical and equal 1.

In the first figure, quantizer has 16 levels. According to this figure three phases can be observed:

- For the additive noise model, when q is small, the power of quantization noise is very low. On the other hand, for the quantizer model, because there is limited number of quantization levels, it can not completely cover the dynamic range of received signal. So the achievable rate for the additive model is higher.

- When q increases the achievable rate obtained from these two models meet each other.

- As q get larger, the power of additive noise still grows and achievable rate decreases monotonically. But in the quantizer model as q increases the whole received signal

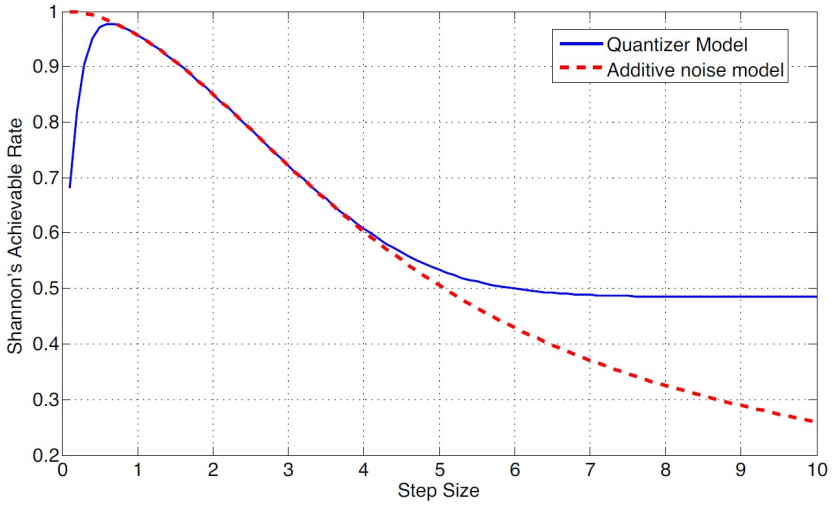

Figure 2.6: Comparison of Shannon's Achievable rate for two models. Number of levels: 16

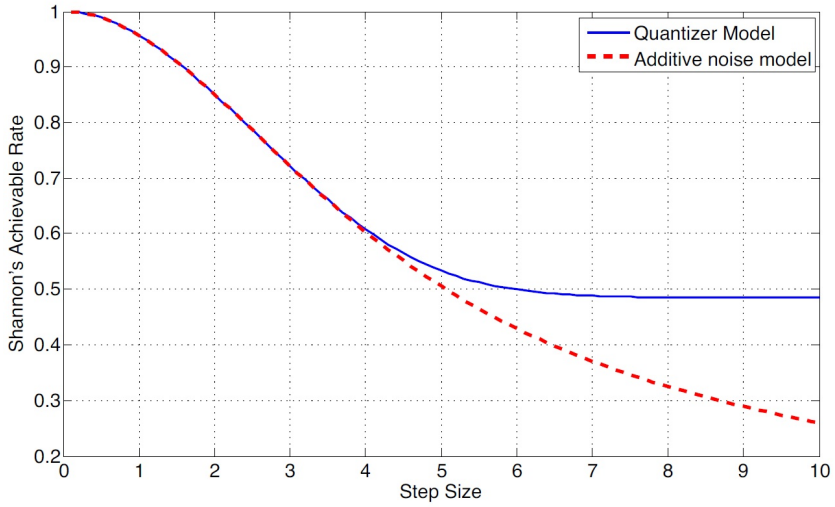

Figure 2.7: Comparison of Shannon's Achievable rate for two models. Number of levels: 128

lies in one quantization bin and the achievable rate saturates, and after this point increasing quantization step size does not change the rate.

In the second figure, we increase number of levels to 128 and nothing else is changed. As we expected the effect of this increment is only on the first phase and the other two phases remain the same as the previous figure.

2.2.4 Reducing Truncation noise

Because quantizers have limited number of bits, their dynamic range can not be infinity. Consequently, the input signal will be clipped if its amplitude is beyond the dynamic range of the quantizer. There is some works ([17]-[21]) on the effect of clipping the OFDM signals and methods of mitigating the clipping error. The well-known effects of clipping OFDM signals are in-band distortion and out-band noise emission.

In this subsection, we assume that the quantizer is fixed and from the receiver point of view try to increase the performance of the system.

Now, consider the receiver at terminal 2 in the Fig. 2.8 (results can be used for the other receiver).

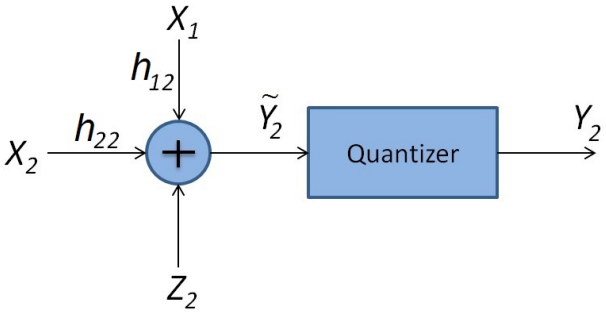

Figure 2.8: Receiver at terminal 2

The desired signal for this receiver is X_1, and X_2 is self-interference. Let's denote the power of X_1 and X_2 by P_1 and P_2 respectively. That is:

$$P_1 = E[{X_1}^2] \qquad P_2 = E[{X_2}^2] \tag{2.32}$$

As we mentioned earlier, at each receiver, power of self-interference signal is much higher than power of desired signal. In the other word $h_{22} \gg h_{12}$. But, X_2 is known for receiver 2. Now we introduce a new random variable, W_2, which is defined as the following:

$$W_2 = h_{12}X_1 + Z_2. \tag{2.33}$$

Since X_1 and Z_2 are two independent Gaussian random variables, we have:

$$P_{W_2} = {h_{12}}^2 P_1 + \sigma_{z_2}^2 \tag{2.34}$$

So we may re-write (2.25) and power of $\tilde{Y_2}$ as follows:

$$\tilde{Y_2} = h_{22}X_2 + W_2 \tag{2.35}$$

$$P_{\tilde{Y_2}} = {h_{22}}^2 P_2 + P_{W_2} \tag{2.36}$$

$\tilde{Y_2}$ goes through a quantizer and whenever its absolute value is greater than T, the truncation point, it's truncated. Let's denote the truncation error in receiver 2 by γ_2. We would like to calculate the power of this error. To do so, we need first to present a formulation. We introduce a new variable, I_T, which takes two values (0 and 1) according to the following expression:

$$I_T(\xi) = \begin{cases} 0 & \text{if } |\xi| \leqslant T, \\ 1 & \text{if } |\xi| > T. \end{cases} \tag{2.37}$$

Using this new variable, the power of γ_2 is defined as:

$$E[{\gamma_2}^2] = \int_{-\infty}^{\infty} I_T(\tilde{Y_2})(\tilde{Y_2} - T)^2 f_{\tilde{Y_2}}(\tilde{y_2}) \mathrm{d}\tilde{y_2}, \tag{2.38}$$

where:

$$f_{\tilde{Y_2}}(\tilde{y_2}) = \frac{1}{\sqrt{2\pi P_{\tilde{Y_2}}}} e^{-\frac{\tilde{y_2}^2}{2P_{\tilde{Y_2}}}} \tag{2.39}$$

The amount of this error power depends on power of quantizer input, $\tilde{Y_2}$, and truncation point, T.

Our method to decrease $E({\gamma_2}^2)$ is based on our knowledge about X_2. Since we know X_2, we can compensate error in truncation to some extend. Suppose we have clipper $\mathcal{C}$ which clips its input signal if its absolute value is larger than T'. We pass $h_{22}X_2$ through $\mathcal{C}$. Now, whenever $\tilde{Y_2} > T$, we check if $h_{22}X_2 > T'$. If this is the case, then we add $h_{22}X_2 - T'$ to T to produce the output of $\mathcal{Q}$. So the output would be $T + (h_{22}X_2 - T')$. Besides, if $\tilde{Y_2} < -T$ and $h_{22}X_2 < -T'$ the output of the quantizer would be $-T - (-h_{22}X_2 - T')$. In this way, we decrease the amount of error. In general, by this method, error γ_2 is as the following:

$$\gamma_2 = \begin{cases} |\tilde{Y_2}| - T & \text{if } \begin{cases} \tilde{Y_2} > T \quad \text{and} \quad h_{22}X_2 < T' \\ \text{or} \\ \tilde{Y_2} < -T \quad \text{and} \quad h_{22}X_2 > -T' \end{cases} \\ |W_2 - T + T'| & \text{if } \tilde{Y_2} > T, \quad \text{and} \quad h_{22}X_2 > T',^{\star}\, 1 \\ |W_2 + T - T'| & \text{if } \tilde{Y_2} < -T, \quad \text{and} \quad h_{22}X_2 < -T.^{\dagger} \\ 0 & \text{otherwise} \end{cases} \tag{2.40}$$

Where $(\star)$ and $(\dagger)$ come from the following expressions:

$(\star)$ if $\tilde{Y_2} > T$ and $h_{22}X_2 > T'$ then the error is: $|\tilde{Y_2} - (T + (h_{22}X_2 - T'))| = |W_2 - T + T'|$

$(\dagger)$ if $\tilde{Y_2} < -T$ and $h_{22}X_2 < -T'$ then the error is:
$|\tilde{Y_2} - (-T - (-h_{22}X_2 - T'))| = |W_2 + T - T'|$

Now, we need to calculate the power of γ_2 based on this new definition and new parameters and find the optimum value of T' which minimizes the error power. We take α

as the ratio of the received power from signal X_2 to the one from W_2 at receiver 2.

$$\alpha = \frac{{h_{22}}^2 P_2}{P_{W_2}} \tag{2.41}$$

Figure 2.9 , shows the result of simulations for the optimum value of T' for different values of T and α. It is clear that for very large T', results are the same as the scenario without clipper $\mathcal{C}$.

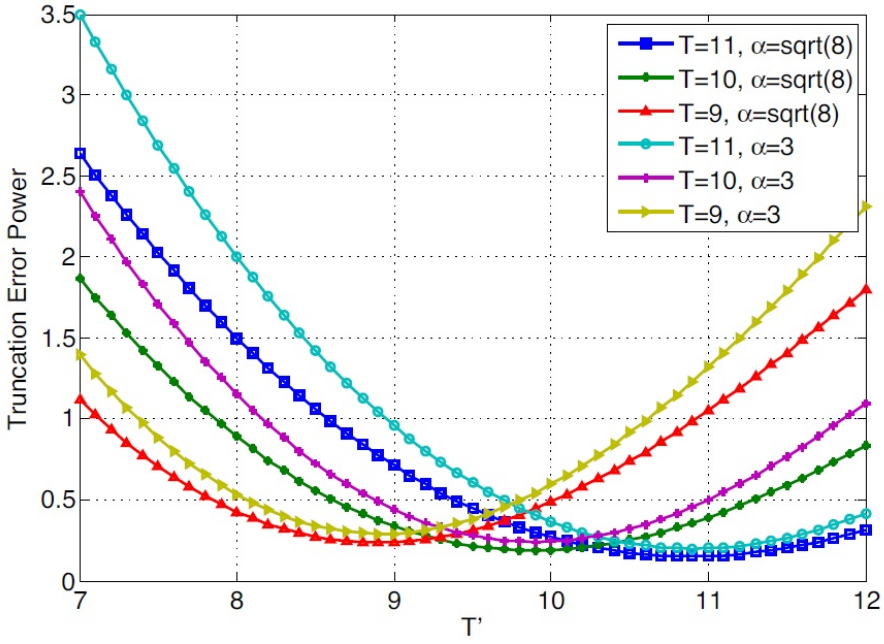

Figure 2.9: Optimum value of T' for different quantizers

2.3 Constellation-based Inputs

Next, we evaluate the Shannon achievable region in a GTWC with constellation-based inputs. In [11] and [12] use of constellation-based input for Gaussian MAC and Gaussian broadcast channel with quantized output is investigated. Simulation results in Table 1

compares the values of R_1 in constellation-based GTWC with PAM signals and GTWC with Gaussian inputs. According to this Table, at least at low SNR discrete input has supremacy over Gaussian. We didn't optimize over all discrete inputs though, and just used identical 8-points PAM with different power constraint for both transmitters. For subsections 2.3.1 to 2.3.4, we assume that the noise power is equal to 1, i.e., $\sigma_z^2 = 1$ and channel gains are symmetrical, i.e., $h_{11} = h_{22}$ and $h_{12} = h_{21}$.

Table 2.1: Performance of Gaussian and Discrete Inputs in a GTWC with Output Quantization

SNR	Gaussian Inputs		Discrete Inputs (PAM)	
	R_1	Opt. step Size	R_1	Opt. step Size
1	0.46432	0.95	0.46972	0.85
2	0.71814	1.2	0.72418	1.05
3	0.88916	1.4	0.89247	1.2
4	1.0162	1.55	1.0165	1.4
5	1.116	1.65	1.1125	1.5
6	1.1976	1.8	1.1911	1.7
7	1.2659	1.9	1.2564	1.8

Suppose X_1 and X_2 are generated uniformly over finite constellations $\mathcal{X}_1$ and $\mathcal{X}_2$ with cardinality K_1 and K_2, respectively, i.e., $\mathcal{X}_i = \{x_{i,1}, x_{i,2}, ..., x_{i,K_i}\}$ for $i \in \{1, 2\}$. One may express $I(X_1; Y_2|X_2)$ as

$$I(X_1; Y_2 \mid X_2) = H(Y_2 \mid X_2) - H(Y_2 \mid X_1, X_2). \tag{2.42}$$

For $I(X_2; Y_1 \mid X_1)$ we will have exactly the same arguments as (2.42) and just need to exchange the indexes.

We study both 1-dimensional and 2-dimensional scenarios in the following subsections.

2.3.1 1-Dimensional Constellations

In this subsection we consider a constellation with points along one axis. For such constellation, $H(Y_2 \mid X_2)$ in (2.42) has the following form:

$$H(Y_2 \mid X_2) = \frac{1}{K_2} \sum_{i=1}^{K_2} H(Y_2 \mid X_2 = x_{2,i}) \tag{2.43}$$

and

$$\begin{gathered} H(Y_2 \mid X_2 = x_{2,i}) = \\ -\sum_{k=1}^{M} P(Y_2 = l_k \mid X_2 = x_{2,i}) \log_2 P(Y_2 = l_k \mid X_2 = x_{2,i}). \end{gathered} \tag{2.44}$$

On the other hand,

$$\begin{gathered} P(Y_2 = l_k \mid X_2 = x_{2,i}) = \\ \frac{1}{K_1} \sum_{j=1}^{K_1} P(Y_2 = l_k \mid X_2 = x_{2,i}, X_1 = x_{1,j}) \end{gathered} \tag{2.45}$$

We need to discuss about (2.45). Note that Y_2 is a quantized version of $\tilde{Y}_2$ and the probability density function of $\tilde{Y}_2$ is

$$f(\tilde{Y}_2 \mid X_2 = x_{2,i}, X_1 = x_{1,j}) = \frac{1}{\sqrt{2\pi}} \exp\left(-\frac{(\tilde{Y}_2 - h_{22}x_{2,i} - h_{12}x_{1,j})^2}{2}\right). \tag{2.46}$$

This leads us to (2.47) where $\phi(\cdot)$ is the cumulative distribution function of a standard Gaussian random variable.

$$\begin{aligned} P(Y_2 = l_k \mid X_2 = x_{2,i}, X_1 = x_{1,j}) &= P(\tilde{Y}_2 \in \mathcal{R}_k \mid X_2 = x_{2,i}, X_1 = x_{1,j}) \\ &= \int_{b_{i-1}}^{b_i} \frac{1}{\sqrt{2\pi}} \exp\left(-\frac{(\tilde{Y}_2 - h_{22}x_{2,i} - h_{12}x_{1,j})^2}{2}\right) d\tilde{Y}_2 \\ &= \phi(b_i - h_{22}x_{2,i} - h_{12}x_{1,j}) - \phi(b_{i-1} - h_{22}x_{2,i} - h_{12}x_{1,j}) \end{aligned} \tag{2.47}$$

As for $H(Y_2 \mid X_1, X_2)$,

$$H(Y_2 \mid X_1, X_2) = \tfrac{1}{K_1}\tfrac{1}{K_2} \sum_{j=1}^{K_1} \sum_{i=1}^{K_2} H(Y_2 \mid X_1 = x_{1,j}, X_2 = x_{2,i}). \tag{2.48}$$

Similarly, $H(Y_2 \mid X_1 = x_{1,j}, X_2 = x_{2,i})$ can be written as follows:

$$\begin{aligned} & H(Y_2 \mid X_1 = x_{1,j}, X_2 = x_{2,i}) \\ & = -\sum_{k=1}^{M} P(Y_2 = l_k \mid X_2 = x_{2,i}, X_1 = x_{1,j}) \log_2 P(Y_2 = l_k \mid X_2 = x_{2,i}, X_1 = x_{1,j}) \end{aligned} \tag{2.49}$$

2.3.2 2-Dimensional Constellations

Next, we consider 2-Dimensional Constellations. The ambient noise at both ends is modeled as circularly symmetric complex Gaussian noise with unit variance.

We require to perform 2-dimensional quantization at outputs. Quantization is performed independently on each dimension. Due to uniform quantization, the quantizer regions, $\mathcal{R}_{mn}$, will be rectangular with horizontal boundaries b_{m-1} and b_m and vertical boundaries d_{n-1} and d_n. Let us denote the quantization regions by l_{mn}. Assume that the quantizers have M horizontal and N vertical levels. If $y_i \in \mathcal{R}_{mn}$ then $Q(y_i) = l_{mn}$ (for $i = 1, 2$). Basically, expressions for obtaining conditional mutual information in 2-dimensional case can be derived in an almost similar manner to 1-dimensional problem. However, they are slightly different. Equations (2.43) and (2.48) remain unchanged. However, equations (2.44) to (2.47) and (2.49) change to equations (2.50) to (2.54) where $V^{(1)}$ and $V^{(2)}$ denote components of variable V, $V = V^{(1)} + \sqrt{-1}V^{(2)}$. Note that we need to rely on numerical computations.

$$H(Y_2 \mid X_2 = x_{2,i}) = -\sum_{m=1}^{M} \sum_{n=1}^{N} P(Y_2 = l_{mn} \mid X_2 = x_{2,i}) \log_2 P(Y_2 = l_{mn} \mid X_2 = x_{2,i}) \tag{2.50}$$

$$P(Y_2 = l_{mn} \mid X_2 = x_{2,i}) = \frac{1}{K_1} \sum_{j=1}^{K_1} P(Y_2 = l_{mn} \mid X_2 = x_{2,i}, X_1 = x_{1,j}) \tag{2.51}$$

$$f(\tilde{Y}_2 \mid X_2 = x_{2,i}, X_1 = x_{1,j}) = \frac{1}{\pi} e^{-|\tilde{Y}_2 - x_{2,i} - x_{1,j}|^2} \tag{2.52}$$

$$\begin{aligned} P(Y_2 = l_{mn} \mid X_2 = x_{2,i}, X_1 = x_{1,j}) &= P(\tilde{Y}_2 \in \mathcal{R}_{mn} \mid X_2 = x_{2,i}, X_1 = x_{1,j}) \\ &= \int_{b_{m-1}}^{b_m} \int_{d_{n-1}}^{d_n} \tfrac{1}{\pi} e^{-|\tilde{Y}_2 - x_{2,i} - x_{1,j}|^2} d\tilde{Y}_2^{(1)} d\tilde{Y}_2^{(2)} \\ &= \Big[\phi(\sqrt{2}(b_m - x_{2,i}^{(1)} - x_{1,j}^{(1)})) - \phi(\sqrt{2}(b_{m-1} - x_{2,i}^{(1)} - x_{1,j}^{(1)}))\Big] \\ &\times \Big[\phi(\sqrt{2}(d_n - x_{2,i}^{(2)} - x_{1,j}^{(2)})) - \phi(\sqrt{2}(d_{n-1} - x_{2,i}^{(2)} - x_{1,j}^{(2)}))\Big] \end{aligned} \tag{2.53}$$

$$\begin{aligned} &H(Y_2 \mid X_1 = x_{1,j}, X_2 = x_{2,i}) \\ &= -\sum_{m=1}^{M} \sum_{n=1}^{N} P(Y_2 = l_{mn} \mid X_2 = x_{2,i}, X_1 = x_{1,j}) \log_2 P(Y_2 = l_{mn} \mid X_2 = x_{2,i}, X_1 = x_{1,j}) \end{aligned} \tag{2.54}$$

In the next subsection, the rate region will be sketched for 4-PAM and QPSK at some SNRs.

2.3.3 Rotation of Constellation

In this section we extend the concept of Uniquely Decodable (UD) alphabet pairs proposed in [24]. For given constellations $\mathcal{X}_1$ and $\mathcal{X}_2$, $\mathcal{X}_{sum1}$ and $\mathcal{X}_{sum2}$ are defined as follow (given

$h_{11} = h_{22} = a$ and $h_{12} = h_{21} = b$):

$$\begin{aligned} \mathcal{X}_{sum1} &= \{Q(ax_1 + bx_2) \mid \forall x_1 \in \mathcal{X}_1, x_2 \in \mathcal{X}_2\} \\ \mathcal{X}_{sum2} &= \{Q(bx_1 + ax_2) \mid \forall x_1 \in \mathcal{X}_1, x_2 \in \mathcal{X}_2\} \end{aligned} \tag{2.55}$$

In fact, $\mathcal{X}_{sum1}$ and $\mathcal{X}_{sum2}$ denote the quantized version of received constellations at each receiver. Given the mappings $\psi_1 : \mathcal{X}_1 \times \mathcal{X}_2 \mapsto \mathcal{X}_{sum1}$ and $\psi_2 : \mathcal{X}_1 \times \mathcal{X}_2 \mapsto \mathcal{X}_{sum2}$, we call the pair $(\mathcal{X}_1, \mathcal{X}_2)$ to be a UD pair if ψ_1 and ψ_2 are one-to-one mappings.

If the pair $(\mathcal{X}_1, \mathcal{X}_2)$ is UD, probability of error in decoding the received signal decreases and information can be transmitted through the channel at higher rates.

A simple way to achieve such UD pairs is to rotate the constellation of one user, i.e, $\mathcal{X}_2 = \mathcal{X}_1 e^{j\theta}$. As such, we let $K_1 = K_2 = K$. Our goal is to find an angle of rotation that maximally enlarges the Shannon achievable region. Let us denote such an angle by θ^*. Numerical simulations show that the rotation of one constellation enlarges the achievable region and in some cases, results in a rectangular region. According to the definition of UD pairs, it is clear that in some cases, constellation rotation does not help us in reaching our goal, i.e., $\theta^* = 0$, specially for quantizers with large step size. In fact, the optimum value of θ depends on the structure of the quantizer. Generally, for 1-dimensional constellations, $\theta^* = 90$ for most of the cases. For 2-dimensional constellation, by increasing the number of constellation points, the optimum angle decreases.

For a UD constellation pair, both $\mathcal{X}_{sum1}$ and $\mathcal{X}_{sum2}$ have K^2 elements. As SNR increases, sum rate converges to $\log_2 K^2 = 2\log_2 K$, which is the maximum achievable sum-rate for a channel with K-point constellations at inputs.

It is necessary to mention that, if we do not quantize the output, rotation of constellation would not help, because the receiver knows the constellation and rotating it does not give any further information. However, since the quantizer does not operate linearly, its output is not completely clear for the receiver. From a mathematical point of view, we can say without quantization (2.53) is an integral from $-\infty$ to $+\infty$ and rotation (which is equivalent to changing the mean value of the random variable $\tilde{Y}_2$) does not have any effect on the results. But, because here we are integrating on a bounded interval, location of the

mean value of $\tilde{Y}_2$ is important.

2.3.4 Applying Rotation method to some known Constellations

In this subsection the effect of rotation of constellation is studied for some practical constellation choices. In all of the results of this section, we assume all channel gains are equal to 1, and step size of the quantizer is also equal to 1.

We first apply this method to a 4-PAM constellation. As it is illustrated in figure 2.10, rotation enlarges the achievable rate region considerably, specially for higher values of SNR. Without rotation we have only one dimension in transmission. Through applying rotation, we are adding another dimension which decreases the effect of self-interference.

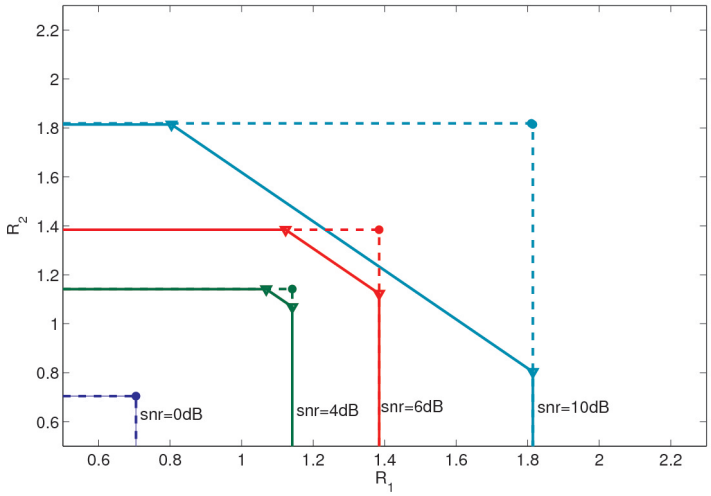

Figure 2.10: Result of Rotation of Constellation for 4-PAM at different SNRs- Dashed: with rotation, Solid: without rotation

Figure 2.11 shows the results of rotation of one QPSK constellation. Here, we can see the advantage of rotation as well. In a moderate SNR (10 dB) we can almost achieve 2 bits/sec/hz for each user which is the maximum achievable rate when we use this particular constellation.

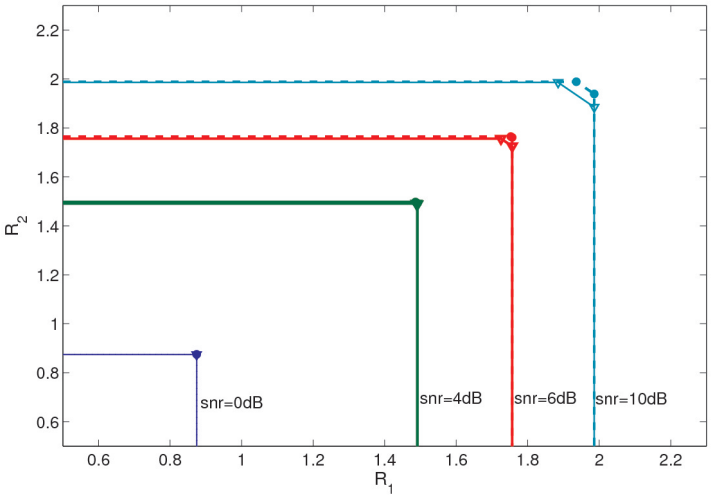

Figure 2.11: Result of Rotation of Constellation for QPSK at different SNRs- Dashed: with rotation, Solid: without rotation

We can also compare the performance of these two constellations. For all amounts of SNR, QPSK works better than PAM, as it was expected. But, for PAM, improvement obtained by rotation of constellation is much larger than QPSK. This is due to the orthogonality ($\theta^* = 90$ for PAM) caused by rotation for 1-dimensional constellations.

2.3.5 Adjusting self-interference channel gain

In this subsection we consider a fixed quantizer at each receiver side, i.e. users are not able to manipulate the structure of output quantizer to obtain a better achievable rate. But, there is another parameter in their hand to play with and achieve a higher rate. Actually, they can adjust the self-interference channel gain. We suppose that each user can adjust the power of signal that goes to its own receiver, but because of some obstacles (such as system inaccuracy or analog-to-digital conversions) they can not completely remove this interference. In other words, each leakage channel gain h_{ii} is always beyond some constant α_i. So $h_{ii} \in [\alpha_i, \infty)$. We would like to show, although the signal from one's node transmitter to its receiver is an interfering signal, due to presence of quantizer at each endpoint, minimizing the power of this signal does not help us to obtain a higher

transmission rate.

We consider K-point PAM as the channel input. Each user uniformly chooses one of these K points to transmit.

Again we work on R_1. We can use expressions in subsection 2.3.1 to calculate the achievable rate. In these expressions every thing is given except h_{22}. We change this parameter to obtain maximum achievable rate. The channel gain at which this maximum rate is achieved is denoted by $h_{22}{}^*$.

Figure below demonstrates the R_1 versus h_{22}. For this simulation we consider a 4-point PAM, forward channel gain is 1 ($h_{12} = 1$), and quantizer has 16 levels with step size equal to 2. According to this figure it is obvious that rate is not a monotone decreasing function of leakage channel gain.

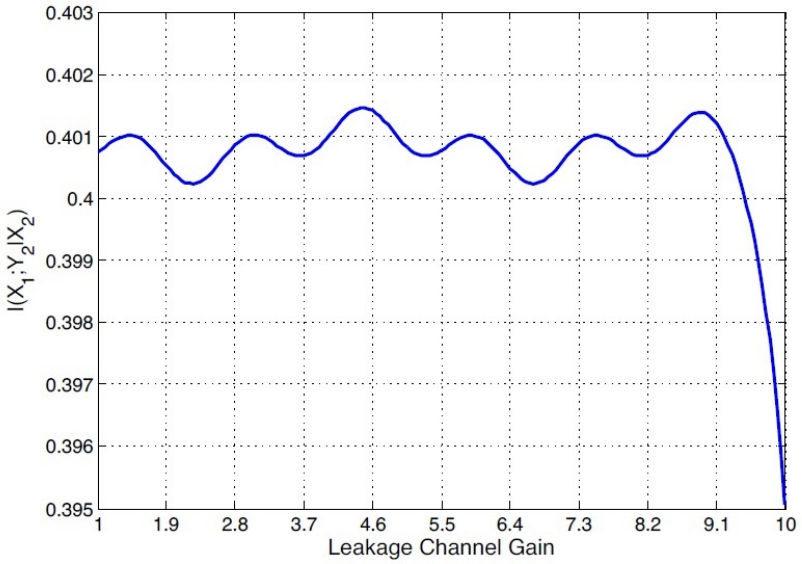

Figure 2.12: Effect of changing leakage channel gain on achievable rate

Figure 2.13 , shows the received constellation at receiver 2, without noise. According to this figure and our other observations, whenever the the received constellation is uniformly placed at quantization bins, the rate increases. This result can be justified by saying that when the points are uniformly placed, they become distinguishable. So the effect of channel

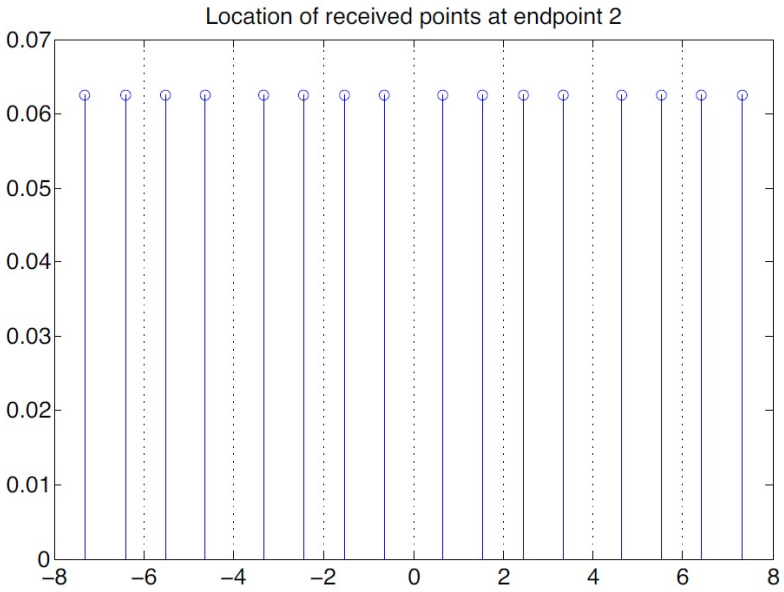

Figure 2.13: location of points before adding noise, the dashed lines are boundaries of quantizer's bins

noise becomes low.

Chapter 3

Gaussain Erasure Two-Way Channel

3.1 Introduction

In this chapter Gaussian Erasure Two-Way channel is studied. In an erasure channel the received signal is erased and the erasure factor has some probability distribution. Under this situation the receiver just receives the channel noise. We will use discrete random variables as the channel inputs. So the pdf of received signal at each endpoint is mixed-Gaussian. Before we start to describe our model in this chapter, a very important and useful theorem is expressed as the following:

Theorem 3.1.1. [1] *Let X be a random variable with PDF*

$$p(x) = \sum_{m=1}^{M} \frac{p_m}{\sqrt{2\pi P}} e^{-\frac{(x-x_m)^2}{2P}}, \tag{3.1}$$

[1] Derived by K. Moshksar, Ph.D. (kmoshksa@uwaterloo.ca), Supposed to be submitted in a joint paper

where $x_1 < \cdots < x_M$ *and* $(p_m)_{m=1}^M$ *is a discrete probability sequence. Define*

$$a_m = p_m e^{-\frac{x_m^2}{2P}},\ b_m = \frac{x_m}{P},\ m = 1, \cdots, M, \tag{3.2}$$

$$c_m^+ = \frac{a_m}{a_M},\ d_m^+ = b_m - b_M,\ m = 1, \cdots, M-1, \tag{3.3}$$

$$c_m^- = \frac{a_m}{a_1},\ d_m^- = b_1 - b_m,\ m = 2, \cdots, M, \tag{3.4}$$

$$\eta^+(x) = \ln\left(1 + \sum_{m=1}^{M-1} c_m^+ e^{d_m^+ x}\right),\ x \in \mathbb{R}_+, \tag{3.5}$$

$$\eta^-(x) = \ln\left(1 + \sum_{m=1}^{M-1} c_m^- e^{d_m^- x}\right),\ x \in \mathbb{R}_+. \tag{3.6}$$

Let $x_*^+ \geq 0$ *be the unique root of* $\eta^+(x) = \ln 2$ *for* $a_M < \frac{1}{2}$ *and* $x_*^+ = 0$ *otherwise. Similarly, let* $x_*^- \geq 0$ *be the unique root of* $\eta^-(x) = \ln 2$ *for* $a_1 < \frac{1}{2}$ *and* $x_*^- = 0$ *otherwise. For any* $N_1^{\mathrm{lb}}, N_1^{\mathrm{ub}}, N_2 \in \mathbb{N} \cup \{0\}$,

$$\beta + \alpha_{2N_1^{\mathrm{lb}}+1, N_2} \leq h(X) \leq \beta + \alpha_{2N_1^{\mathrm{ub}}, N_2}, \tag{3.7}$$

where $\alpha_{N,N'}$ *and* β *are given in (3.8) and (3.9), respectively. Finally, the errors* $\alpha_{2N_1^{\mathrm{ub}}, N_2} + \beta - h(X)$ *and* $\alpha_{2N_1^{\mathrm{lb}}+1, N_2} + \beta - h(X)$ *scale like* $O\left(\frac{1}{N_1^{\mathrm{ub}}}\right) + O\left(\frac{1}{N_2}\right)$ *and* $O\left(\frac{1}{N_1^{\mathrm{lb}}}\right) + O\left(\frac{1}{N_2}\right)$, *respectively.*

Proof. See appendix A. □

This theorem helps us to find arbitrarily tight bounds on the entropy of a Mixed-Gaussian random variables.

$$
\begin{aligned}
\alpha_{N,N'} &:= \log e \sum_{n=1}^{N} \frac{(-1)^n}{n} \sum_{\substack{j_1,\cdots,j_{M-1}\geq 0 \\ j_1+\cdots+j_{M-1}=n}} \frac{n!}{\prod_{m=1}^{M-1} j_m!} \theta^+(j_1,\cdots,j_{M-1}) \prod_{m=1}^{M-1} (c_m^+)^{j_m} \\
&\quad + \log e \sum_{n=1}^{N} \frac{(-1)^n}{n} \sum_{\substack{j_2,\cdots,j_M\geq 0 \\ j_2+\cdots+j_M=n}} \frac{n!}{\prod_{m=2}^{M} j_m!} \theta^-(j_2,\cdots,j_M) \prod_{m=2}^{M} (c_m^-)^{j_m} \\
&\quad - \log e \sum_{n=0}^{N'-1} \sum_{m=1}^{M} p_m \eta^+(x_n^+) \left(Q\left(\frac{x_n^+ - x_m}{\sqrt{P}} \right) - Q\left(\frac{x_{n+1}^+ - x_m}{\sqrt{P}} \right) \right) \\
&\quad - \log e \sum_{n=0}^{N'-1} \sum_{m=1}^{M} p_m \eta^-(x_n^-) \left(Q\left(\frac{x_n^- + x_m}{\sqrt{P}} \right) - Q\left(\frac{x_{n+1}^- + x_m}{\sqrt{P}} \right) \right). \qquad (3.8)
\end{aligned}
$$

$$
\begin{aligned}
\beta &:= \frac{1}{2}\log(2\pi P) + \frac{\log e}{2P}\left(P + \sum_{m=1}^{M} p_m x_m^2 \right) \\
&\quad - \log a_M \sum_{m=1}^{M} p_m Q\left(-\frac{x_m}{\sqrt{P}} \right) - \log a_1 \sum_{m=1}^{M} p_m Q\left(\frac{x_m}{\sqrt{P}} \right) \\
&\quad - \log e\, b_M \sum_{m=1}^{M} p_m \left(\sqrt{\frac{P}{2\pi}} e^{-\frac{x_m^2}{2P}} + x_m Q\left(-\frac{x_m}{\sqrt{P}} \right) \right) \\
&\quad - \log e\, b_1 \sum_{m=1}^{M} p_m \left(x_m Q\left(\frac{x_m}{\sqrt{P}} \right) - \sqrt{\frac{P}{2\pi}} e^{-\frac{x_m^2}{2P}} \right). \qquad (3.9)
\end{aligned}
$$

$$
\theta^{\pm}(j_1,\cdots,j_{M-1}) := \sum_{s=1}^{M} a_s\, e^{\frac{1}{2}P\left(\pm b_s + \sum_{m=1}^{M-1} j_m d_m^{\pm}\right)^2} Q\left(\frac{1}{\sqrt{P}} \left(x_*^{\pm} - P\left(\pm b_s + \sum_{m=1}^{M-1} j_m d_m^{\pm} \right) \right) \right) \qquad (3.10)
$$

$$
x_n^+ := \frac{n x_*^+}{N_2},\ x_n^- := \frac{n x_*^-}{N_2},\ n = 0,\cdots,N_2. \qquad (3.11)
$$

3.2 System Model

Let us consider a two-way channel where the received signal at endpoints 1 and 2 are given by

$$Y_1 = E_1(h_{11}X_1 + h_{21}X_2) + Z_1 \tag{3.12}$$

and

$$Y_2 = E_2(h_{12}X_1 + h_{22}X_2) + Z_2, \tag{3.13}$$

respectively. Here, $X_k \in \mathcal{X}_k = \{-\sqrt{P_k}, \sqrt{P}_k\}$ are such that

$$\Pr\{X_k = x\} = \frac{1}{2},\ x \in \mathcal{X}_k,\ k = 1, 2. \tag{3.14}$$

This yields

$$E[X_k] = 0,\ \ E[X_k^2] = P_k,\ \ k = 1, 2. \tag{3.15}$$

Moreover, Z_1 and Z_2 are independent $\mathrm{N}(0, 1)$ random variables and E_1 and E_2 are independent $\mathrm{Ber}(\mathsf{e}_1)$ and $\mathrm{Ber}(\mathsf{e}_2)$ random variables, respectively, for known $\mathsf{e}_1, \mathsf{e}_2 \in (0, 1)$ at both ends. We emphasize that E_1 and E_2 are unknown to both ends. The gain $h_{i,i}$ can be set at any value in $[\alpha_i, \infty)$ for $i = 1, 2$.

3.3 Shannon achievable rate in Gaussian Erasure Two-Way channel with binary input

We know that the Shannon achievable rate is given by

$$R_1 \le R_1^* := I(X_2; Y_1|X_1),\ \ R_2 \le R_2^* := I(X_1; Y_2|X_2). \tag{3.16}$$

We have

$$R_1^* := h(Y_1|X_1) - h(Y_1|X_1, X_2), \tag{3.17}$$

where

$$h(Y_1|X_1) = \frac{1}{2}\sum_{x_1\in\mathcal{X}_1} h(E_1(h_{11}x_1 + h_{21}X_2) + Z_1) \tag{3.18}$$

and

$$h(Y_1|X_1, X_2) = \frac{1}{4}\sum_{x_1\in\mathcal{X}_1, x_2\in\mathcal{X}_2} h(E_1(h_{11}x_1 + h_{21}x_2) + Z_1). \tag{3.19}$$

To calculate $h(E_1(h_{11}x_1 + h_{21}X_2) + Z_1)$ note that $E_1(h_{11}x_1 + h_{21}X_2) + Z_1$ is a mixed Gaussian random variable where all its Gaussian components have unit variance and means 0, $h_{11}x_1 - h_{21}\sqrt{P_2}$ and $h_{11}x_1 + h_{21}\sqrt{P_2}$ with corresponding probabilities $1-\mathsf{e}_1$, $\frac{\mathsf{e}_1}{2}$ and $\frac{\mathsf{e}_1}{2}$. Also, in computing $h(E_1(h_{11}x_1 + h_{21}x_2) + Z_1)$, we note that $E_1(h_{11}x_1 + h_{21}x_2) + Z_1$ is a mixed Gaussian random variable where both its Gaussian components have unit variance and means 0, $h_{11}x_1+h_{21}x_2$ with corresponding probabilities $1-\mathsf{e}_1$ and e_1. As such, Theorem 1 can be utilized to derive arbitrarily tight upper and lower bounds on R_1^*.

For example, let us consider a scenario where $\alpha_1 = \alpha_2 = 1$, $h_{1,2} = h_{2,1} = 1$ and $P_1 = P_2 = 2$dB. Setting $h_{1,1} = h_{2,2} = a$, Fig. 3.1(a) and Fig. 3.1(b) present plots of lower and upper bounds on $R_1^* + R_2^*$ in terms of a for $(\mathsf{e}_1, \mathsf{e}_2) = (0.4, 0.2)$ and $(\mathsf{e}_1, \mathsf{e}_2) = (0.8, 0.7)$, respectively. Setting $N^{(\mathrm{lb})} = 5$ and $N^{(\mathrm{ub})} = 6$ guarantees a uniform distance of less than 0.01 between the upper and lower bounds on $R_1^* + R_2^*$. Moreover, it is seen that $R_1^* + R_2^*$ is an increasing function of a and eventually saturates as a grows sufficiently.

The previous example motivates us to study the behaviour of $R_1^* + R_2^*$ in the large leakage regime where $h_{1,1} = h_{2,2} = a$ tends to infinity. As a increases, the k^{th} user is enable to recognize the realization of E_k. As such the achievable rate for the k^{th} user increases to $I(X_2; Y_1|X_1, E_1)$ that is larger than $I(X_2; Y_1|X_1, E_1)$[2]. To explore this in more detail, let us define[3]

$$U_1(x_1) := E_1(ax_1 + h_{2,1}X_2) + Z_1,\ x_1 \in \mathcal{X}_1 \tag{3.20}$$

and

$$V_1(x_1, x_2) := E_1(ax_1 + h_{2,1}x_2) + Z_1,\ x_k \in \mathcal{X}_k,\ k = 1, 2. \tag{3.21}$$

[2]Note that $I(X_2; Y_1|X_1, E_1) = h(X_2) - h(X_2|Y_1, X_2, E_1)$ that is larger than $h(X_2) - h(X_2|Y_1, X_2) = I(X_2; Y_1|X_1)$ due to the fact that conditioning reduces differential entropy.

[3]The random variables $U_2(x_2)$ and $V_2(x_1, x_2)$ are similarly defined for $x_k \in \mathcal{X}_k,\ k = 1, 2$.

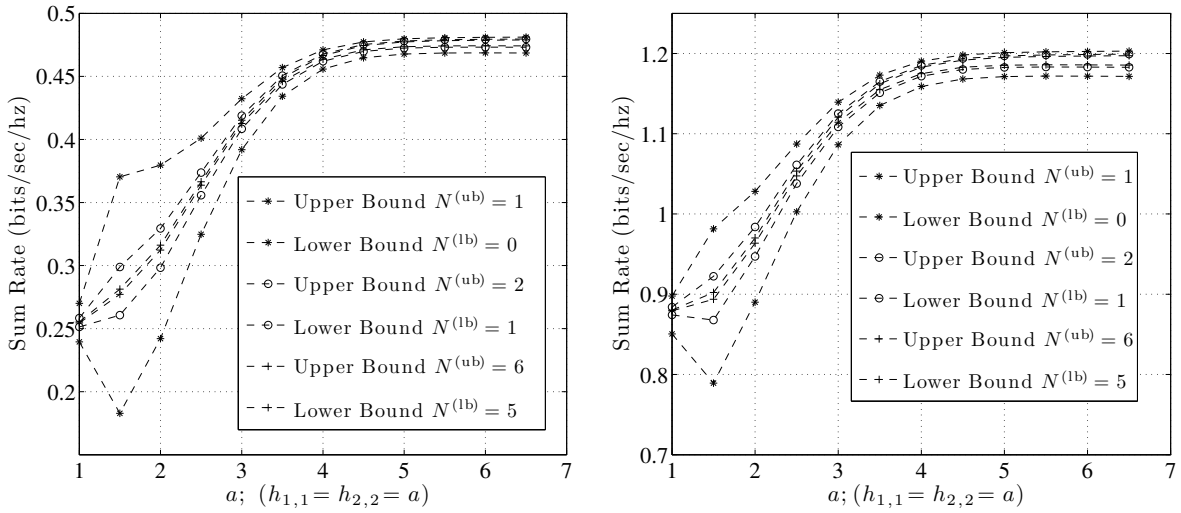

(a) $\mathsf{e}_1 = 0.4, \mathsf{e}_2 = 0.2$ (b) $\mathsf{e}_1 = 0.8, \mathsf{e}_2 = 0.7$

Figure 3.1: Plots of lower and upper bounds on the sum rate $R_1^* + R_2^*$ in a scenario where $h_{1,2} = h_{2,1} = 1$ and $P_1 = P_2 = 2$dB. It is seen that the bounds meet as the indices N_1^{lb} and N_1^{ub} increase.

Then

$$R_1^* = \frac{1}{2} \sum_{x_1 \in \mathcal{X}_1} h(U_1(x_1)) - \frac{1}{4} \sum_{x_1 \in \mathcal{X}_1, x_2 \in \mathcal{X}_2} h(V_1(x_1, x_2)). \tag{3.22}$$

If a is sufficiently large, then $p_{U_1(x_1)|E_1}(u|0) p_{U_1(x_1)|E_1}(u|1) \approx 0$. This together with the fact that $p_{U_1(x_1)}(u) = (1 - \mathsf{e}_1) p_{U_1(x_1)|E_1}(u|0) + \mathsf{e}_1 p_{U_1(x_1)|E_1}(u|1)$ yields

$$\begin{aligned} h(U_1(x_1)) &\approx h(U_1(x_1)|E_1) \\ &= \mathsf{e}_1 h(a x_1 + h_{2,1} X_2 + Z_1) + (1 - \mathsf{e}_1) h(Z_1) \\ &= \mathsf{e}_1 h(h_{2,1} X_2 + Z_1) + (1 - \mathsf{e}_1) h(Z_1) \\ &= \mathsf{e}_1 h(h_{2,1} X_2 + Z_1) + \frac{1 - \mathsf{e}_1}{2} \log(2\pi e), \end{aligned} \tag{3.23}$$

for any $x_1 \in \mathcal{X}_1$. Similarly, for sufficiently large a, we have $p_{V_1(x_1,x_2)|E_1}(v|0) p_{V_1(x_1,x_2)|E_1}(v|1) \approx$

0. Then

$$\begin{aligned} h(V_1(x_1,x_2)) &\approx h(V_1(x_1,x_2)|E_1) \\ &= \mathsf{e}_1 h(ax_1 + h_{2,1}x_2 + Z_1) + (1-\mathsf{e}_1)h(Z_1) \\ &= \mathsf{e}_1 h(Z_1) + (1-\mathsf{e}_1)h(Z_1) \\ &= h(Z_1) \\ &= \frac{1}{2}\log(2\pi e), \end{aligned} \tag{3.24}$$

for any $x_k \in \mathcal{X}_k,\ k = 1, 2$. By (3.22), (3.23) and (3.24),

$$R_1^* \approx \widetilde{R}_1^* := \mathsf{e}_1 h(h_{2,1}X_2 + Z_1) - \frac{\mathsf{e}_1}{2}\log(2\pi e). \tag{3.25}$$

Similarly,

$$R_2^* \approx \widetilde{R}_2^* := \mathsf{e}_2 h(h_{1,2}X_1 + Z_2) - \frac{\mathsf{e}_2}{2}\log(2\pi e). \tag{3.26}$$

Hence, we come up with an approximation for the sum rate given by

$$\widetilde{R}_1^* + \widetilde{R}_2^* = \mathsf{e}_1 h(h_{2,1}X_2 + Z_1) + \mathsf{e}_2 h(h_{1,2}X_1 + Z_2) - \frac{\mathsf{e}_1 + \mathsf{e}_2}{2}\log(2\pi e). \tag{3.27}$$

Note that $h_{2,1}X_2 + Z_1$ and $h_{1,2}X_1 + Z_2$ are mixed Gaussian random variables with densities

$$p_{h_{2,1}X_2+Z_1}(w) = \frac{1}{2}\left(\mathrm{g}(w; -h_{2,1}\sqrt{P_2}, 1) + \mathrm{g}(w; h_{2,1}\sqrt{P_2}, 1)\right) \tag{3.28}$$

and

$$p_{h_{1,2}X_1+Z_2}(w) = \frac{1}{2}\left(\mathrm{g}(w; -h_{1,2}\sqrt{P_1}, 1) + \mathrm{g}(w; h_{1,2}\sqrt{P_1}, 1)\right), \tag{3.29}$$

respectively. It is worth mentioning that in this case the bounds offered in Theorem 1 take on a very simple form. For example,

$$\beta + \alpha_{2N^{(\mathrm{lb})}+1,0} \le h(h_{2,1}X_2 + Z_1) \le \beta + \alpha_{2N^{(\mathrm{ub})},0}, \tag{3.30}$$

where β is given by (3.9),

$$\alpha_{N,0} = \log e \sum_{n=1}^{N} \frac{(-1)^n}{n} \theta(n), \quad N \in \mathbb{N} \tag{3.31}$$

and

$$\theta(n) := e^{2h_{2,1}^2 P_2 n(n-1)} Q\left(h_{2,1}\sqrt{P_2}(2n-1)\right) + e^{2h_{2,1}^2 P_2 n(n+1)} Q\left(h_{2,1}\sqrt{P_2}(2n+1)\right). \tag{3.32}$$

Let us consider a symmetric scenario where $\mathsf{e}_1 = \mathsf{e}_2 = \mathsf{e}$ and $h_{1,2} = h_{2,1} = b$. Then

$$\widetilde{R}_1^* + \widetilde{R}_2^* = \mathsf{e}\left(2h(bX_1 + Z_2) - \log(2\pi e)\right), \tag{3.33}$$

where we have used the fact that $h(bX_1 + Z_2) = h(bX_2 + Z_1)$.

Chapter 4

Conclusion and Future Works

Two-way channel, as an important type of communication channels, has not been well investigated by researchers in the past years. In this thesis, some aspect of two-way channel was studied.

We presented the previous work which have been on this area by other researchers. We explained the inner and outer bounds on the capacity region of the channel and then introduced our models.

In the first part, to get closer to the real world of communication, we considered a two-way channel in which we add a uniform quantizer at both receiver ends. Then we employed both Gaussian and discrete inputs. For Gaussian input, we derived the best step size of the uniform output quantizer that maximizes the Shannon achievable rate. We also evaluate the uniform distribution for the additive quantizer noise from an information theoretic point of view. Then we tried to find a way to reduce the effect of noise that is generated due to presence of quantizer. We split this noise into two parts: Quantization noise and truncation noise and for both of them introduce a way for decreasing the noise impact on the system. For the constellation-based input, like Gaussian input, using numerical method we first obtained the best uniform quantizer at receiver. Then for both 1-dimensional and 2-dimensional constellations we derived the expression of Shannon achievable rate. Then we employed the idea of rotation of one constellation with respect to the other one to

enlarge the Shannon achievable rate region. We observed that using this method, in some cases, the rate region significantly enlarges. At the end of this part, we assumed that each user is able to control the power of self-interference. Actually user can adjust the channel gain between its own receiver and transmitter (but user cannot completely cancel it). Then we showed that in this condition, minimizing the self-interference power is not necessarily a solution for the problem of maximizing the achievable rate.

In the second part we analyzed the Gaussian Erasure Two-Way Channel with discrete input. In this scenario, we chosen a similar approach to the previous section to show that when we are able to set the self-interference channel gain, we need to be aware that we do not always need to decrease this gain as much as possible. Specifically in this case, we can asymptotically understand the erasure factor by increasing the self-interference channel gain.

Contrary to the most communication channel types, such as interference channel, multiple-access channel, broadcast channel,..., Two-way channel has not been studied deeply. There is lots of open problem in this area that can be look at. For example finding the best input distribution for this channel when we are using output quantization is an interesting one.

We believe, as the need of having high-speed communication increases, two-way channel will be one of the most attractive problems among researchers in the field of network information theory.

APPENDICES

Appendix A

One can write $p(\cdot)$ as

$$p(x) = \mathrm{g}(x; P) \sum_{m=1}^{M} a_m e^{b_m x}, \tag{4.1}$$

where $\mathrm{g}(x; P) = \frac{1}{\sqrt{2\pi P}} e^{-\frac{x^2}{2P}}$. It is easy to see that

$$\begin{aligned} \int p(x) \ln p(x) \mathrm{d}x = -\frac{1}{2} \ln(2\pi P) - \frac{E[X^2]}{2P} + \Pr\{X > 0\} \ln a_M \\ + \Pr\{X < 0\} \ln a_1 + b_M E[X \mathbf{1}(X > 0)] + b_1 E[X \mathbf{1}(X < 0)] \\ + \int_0^\infty p(x) \eta^+(x) \mathrm{d}x + \int_0^\infty p(-x) \eta^-(x) \mathrm{d}x. \end{aligned} \tag{4.2}$$

Straightforward calculations show that

$$E[X^2] = P + \sum_{m=1}^{M} p_m x_m^2, \tag{4.3}$$

$$\Pr\{X > 0\} = \sum_{m=1}^{M} p_m Q\left(-\frac{x_m}{\sqrt{P}}\right), \tag{4.4}$$

and

$$\Pr\{X<0\}=\sum_{m=1}^{M}p_m Q\left(\frac{x_m}{\sqrt{P}}\right). \tag{4.5}$$

Moreover,

$$E[X\mathbf{1}(X>0)]=\sum_{m=1}^{M}p_m\left(\sqrt{\frac{P}{2\pi}}e^{-\frac{x_m^2}{2P}}+x_m Q\left(-\frac{x_m}{\sqrt{P}}\right)\right) \tag{4.6}$$

and

$$E[X\mathbf{1}(X<0)]=\sum_{m=1}^{M}p_m\left(x_m Q\left(\frac{x_m}{\sqrt{P}}\right)-\sqrt{\frac{P}{2\pi}}e^{-\frac{x_m^2}{2P}}\right). \tag{4.7}$$

Next, let us consider the term $\int_0^\infty p(x)\eta^+(x)\mathrm{d}x$. We write

$$\int_0^\infty p(x)\eta^+(x)\mathrm{d}x=\int_0^{x_*^+}p(x)\eta^+(x)\mathrm{d}x+\int_{x_*^+}^\infty p(x)\eta^+(x)\mathrm{d}x. \tag{4.8}$$

We treat the integrals in (4.8) separately.

1- For $x>x_*^+$, we have $\sum_{m=1}^{M-1}c_m^+e^{d_m^+x}<1$. Therefore, applying Leibniz test[1] for alternating series and for any $N_1^{\mathrm{lb}}\in\mathbb{N}\cup\{0\}$,

$$\eta^+(x)\le\sum_{n=1}^{2N_1^{\mathrm{lb}}+1}\frac{(-1)^{n-1}}{n}\left(\sum_{m=1}^{M-1}c_m^+e^{d_m^+x}\right)^n \tag{4.9}$$

and the difference between the right and left side in (4.9) is less than or equal to:

$$\frac{1}{2(N_1^{\mathrm{lb}}+1)}\left(\sum_{m=1}^{M-1}c_m^+e^{d_m^+x}\right)^{2(N_1^{\mathrm{lb}}+1)}.$$

[1] An alternating series $\sum_{n=1}^{\infty}(-1)^{n-1}a_n$ where $a_n>0$ converges if a_n is decreasing and $\lim_{n\to\infty}a_n=0$. Moreover, for any $N\in\mathbb{N}$, $\sum_{n=1}^{2N}(-1)^{n-1}a_n\le\sum_{n=1}^{\infty}(-1)^{n-1}a_n\le\sum_{n=1}^{2N+1}(-1)^{n-1}a_n$.

This yields

$$\begin{aligned} 0 \;\leq\; & \sum_{n=1}^{2N_1^{\mathrm{lb}}+1} \frac{(-1)^{n-1}}{n} \int_{x_*^+}^{\infty} p(x) \left(\sum_{m=1}^{M-1} c_m^+ e^{d_m^+ x} \right)^n \mathrm{d}x \\ & - \int_{x_*^+}^{\infty} p(x) \eta^+(x) \mathrm{d}x \\ \leq\; & \frac{1}{2(N_1^{\mathrm{lb}}+1)} \int_{x_*^+}^{\infty} p(x) \left(\sum_{m=1}^{M-1} c_m^+ e^{d_m^+ x} \right)^{2(N_1^{\mathrm{lb}}+1)} \mathrm{d}x. \end{aligned} \tag{4.10}$$

Similarly, for any $N_1^{\mathrm{ub}} \in \mathbb{N}$,

$$\begin{aligned} 0 \;\leq\; & \int_{x_*^+}^{\infty} p(x) \eta^+(x) \mathrm{d}x \\ & - \sum_{n=1}^{2N_1^{\mathrm{ub}}} \frac{(-1)^{n-1}}{n} \int_{x_*^+}^{\infty} p(x) \left(\sum_{m=1}^{M-1} c_m^+ e^{d_m^+ x} \right)^n \mathrm{d}x \\ \leq\; & \frac{1}{2N_1^{\mathrm{ub}}+1} \int_{x_*^+}^{\infty} p(x) \left(\sum_{m=1}^{M-1} c_m^+ e^{d_m^+ x} \right)^{2N_1^{\mathrm{ub}}+1} \mathrm{d}x. \end{aligned} \tag{4.11}$$

It is remarkable that the right side of (4.10) is less than or equal to $\frac{1}{2N_1^{\mathrm{ub}}+1}$ which is $O\left(\frac{1}{N_1^{\mathrm{ub}}}\right)$. This implies that the upper and lower bounds derived on $\int_{x_*^+}^{\infty} p(x)\eta(x)\mathrm{d}x$ are asymptotically tight. One may calculate the terms $\int_{x_*^+}^{\infty} p(x) \left(\sum_{m=1}^{M-1} c_m^+ e^{d_m^+ x}\right)^n \mathrm{d}x$ for any $n \in \mathbb{N}$ as in (4.12).

2- Note that $\eta^+(\cdot)$ is a decreasing function on $[0, \infty)$. Let us show that $\eta^+(\cdot)$ is also convex on $[0, \infty)$. One can write $\left(1 + \sum_{m=1}^{M-1} c_m^+ e^{d_m^+ x}\right) \frac{\mathrm{d}^2}{\mathrm{d}x^2} \eta^+(x)$ as in (4.14). Using Cauchy-

$$\int_{x_*^+}^{\infty} p(x) \left(\sum_{m=1}^{M-1} c_m^+ e^{d_m^+ x} \right)^n \mathrm{d}x = \tag{4.12}$$
$$\sum_{\substack{j_1,\cdots,j_{M-1}\geq 0 \\ j_1+\cdots+j_{M-1}=n}} \frac{n!}{\prod_{m=1}^{M-1} j_m!} \left(\prod_{m=1}^{M-1} \left(c_m^+\right)^{j_m} \right) \int_{x_*^+}^{\infty} p(x) e^{\sum_{m=1}^{M-1} j_m d_m^+ x} \mathrm{d}x,$$

$$\int_{x_*^+}^{\infty} p(x) e^{\sum_{m=1}^{M-1} j_m d_m^+ x} \mathrm{d}x = \tag{4.13}$$
$$\sum_{s=1}^{M} a_s \, e^{\frac{1}{2} P \left(b_s + \sum_{m=1}^{M-1} j_m d_m^+\right)^2} Q\left(\frac{1}{\sqrt{P}} \left(x_*^+ - P\left(b_s + \sum_{m=1}^{M-1} j_m d_m^+ \right) \right) \right).$$

$$\begin{aligned} \left(1 + \sum_{m=1}^{M-1} c_m^+ e^{d_m^+ x} \right) \frac{\mathrm{d}^2}{\mathrm{d}x^2} \eta^+(x) &= \sum_{m=1}^{M-1} c_m^+ (d_m^+)^2 e^{d_m^+ x} + \left(\sum_{m=1}^{M-1} c_m^+ (d_m^+)^2 e^{d_m^+ x} \right) \left(\sum_{m=1}^{M-1} c_m^+ e^{d_m^+ x} \right) \\ &\quad - \left(\sum_{m=1}^{M-1} c_m^+ d_m^+ e^{d_m^+ x} \right)^2 . \end{aligned} \tag{4.14}$$

Schwartz inequality and noting that $c_m > 0$, and we this expression:

$$\left(\sum_{m=1}^{M-1} c_m^+ d_m^+ e^{d_m^+ x}\right)^2 = \left(\sum_{m=1}^{M-1} \left((c_m^+)^{\frac{1}{2}} d_m^+ e^{\frac{1}{2} d_m^+ x}\right)\left((c_m^+)^{\frac{1}{2}} e^{\frac{1}{2} d_m^+ x}\right)\right)^2 \tag{4.15}$$
$$\leq \left(\sum_{m=1}^{M-1} c_m^+ (d_m^+)^2 e^{d_m^+ x}\right)\left(\sum_{m=1}^{M-1} c_m^+ e^{d_m^+ x}\right).$$

Applying this in (4.14) yields $\frac{\mathrm{d}^2}{\mathrm{d}x^2}\eta^+(x) > 0$ for any $x \in \mathbb{R}$, i.e., $\eta^+(\cdot)$ is convex.

We partition the interval $[0, x_*^+]$ into N_2 subintervals with end-points $x_n^+ = \frac{n x_*^+}{N_2}$ for $n = 0, \cdots, N_2$. Define

$$\underline{\eta}(x) := \sum_{n=0}^{N_2-1} \eta^+(x_{n+1}^+)\mathbf{1}(x_n^+ \leq x < x_{n+1}^+) \tag{4.16}$$

and

$$\overline{\eta}(x) := \sum_{n=0}^{N_2-1} \eta^+(x_n^+)\mathbf{1}(x_n^+ \leq x < x_{n+1}^+) \tag{4.17}$$

for $x \in [0, x_*^+]$. Then

$$\underline{\eta}(x) \leq \eta^+(x) \leq \overline{\eta}(x), \quad x \in [0, x_*^+], \tag{4.18}$$

and we get

$$\begin{aligned} \int_0^{x_*^+} p(x)\eta^+(x)\mathrm{d}x &\leq \int_0^{x_*^+} p(x)\overline{\eta}(x)\mathrm{d}x \\ &= \sum_{n=0}^{N_2-1} \eta^+(x_n^+) \int_{x_n^+}^{x_{n+1}^+} p(x)\mathrm{d}x. \end{aligned} \tag{4.19}$$

Similarly,

$$\begin{aligned}\int_0^{x_*^+} p(x)\eta^+(x)\mathrm{d}x &\geq \int_0^{x_*^+} p(x)\underline{\eta}(x)\mathrm{d}x \\ &= \sum_{n=0}^{N_2-1} \eta(x_{n+1}^+)\int_{x_n^+}^{x_{n+1}^+} p(x)\mathrm{d}x.\end{aligned} \tag{4.20}$$

The term $\int_{x_n^+}^{x_{n+1}^+} p(x)\mathrm{d}x$ can be expressed as $\sum_{m=1}^{M} p_m\left(Q\left(\frac{x_n^+-x_m}{\sqrt{P}}\right)-Q\left(\frac{x_{n+1}^+-x_m}{\sqrt{P}}\right)\right)$. To bound the difference $\int_0^{x_*^+} p(x)\overline{\eta}(x)\mathrm{d}x-\int_0^{x_*^+} p(x)\eta^+(x)\mathrm{d}x$, note that $\overline{\eta}(x)-\eta^+(x)\leq \eta^+(x_n)-\eta^+(x_{n+1})$ for $x\in[x_n^+,x_{n+1}^+]$. Hence,

$$\begin{aligned}0 &\leq \int_0^{x_*^+} p(x)\overline{\eta}(x)\mathrm{d}x-\int_0^{x_*^+} p(x)\eta^+(x)\mathrm{d}x \\ &\leq \sum_{n=0}^{N_2-1}\left(\eta^+(x_n)-\eta^+(x_{n+1})\right)\int_{x_n^+}^{x_{n+1}^+} p(x)\mathrm{d}x.\end{aligned} \tag{4.21}$$

The upper bound $\sum_{n=0}^{N_2-1}(\eta^+(x_n^+)-\eta^+(x_{n+1}^+))\int_{x_n^+}^{x_{n+1}^+} p(x)\mathrm{d}x$ tends to 0 as N_2 grows to infinity. To see this note that by the Mean Value Theorem, there are $y_n\in(x_n^+,x_{n+1}^+)$ and $z_n\in(x_n^+,x_{n+1}^+)$ such that

$$\eta^+(x_n^+)-\eta^+(x_{n+1}^+)=-\frac{\mathrm{d}}{\mathrm{d}x}\eta(y_n)(x_{n+1}^+-x_n^+)=-\frac{x_*^+\frac{\mathrm{d}}{\mathrm{d}x}\eta^+(y_n)}{N_2} \tag{4.22}$$

and

$$\int_{x_n^+}^{x_{n+1}^+} p(x)\mathrm{d}x=p(z_n)(x_{n+1}^+-x_n^+)=\frac{x_*^+p(z_n)}{N_2}. \tag{4.23}$$

Therefore, $\sum_{n=0}^{N_2-1}(\eta^+(x_n^+)-\eta^+(x_{n+1}^+))\int_{x_n^+}^{x_{n+1}^+} p(x)\mathrm{d}x$ is equal to $\sum_{n=0}^{N_2-1}\frac{(x_*^+)^2\left(-\frac{\mathrm{d}}{\mathrm{d}x}\eta(y_n)\right)p(z_n)}{N_2^2}$. Since $p(\cdot)$ and $-\frac{\mathrm{d}}{\mathrm{d}x}\eta^+(\cdot)$ are continuous on $[0,x_*^+]$, there are constants $k_1,k_2\in\mathbb{R}_+$ such

that $-\frac{\mathrm{d}}{\mathrm{d}x}\eta^+(y_n) \leq k_1$ and $p(z_n) \leq k_2$ for all values of n. This yields

$$\sum_{n=0}^{N_2-1} (\eta^+(x_n^+) - \eta^+(x_{n+1}^+)) \int_{x_n^+}^{x_{n+1}^+} p(x)\mathrm{d}x \leq \frac{k_1 k_2 (x_*^+)^2}{N_2}, \tag{4.24}$$

which approaches 0 as N_2 tends to infinity. Similarly, we can show that the difference between both sides of (4.24) is $O(N_2^{-1})$.

Finally, note that $\int_{-\infty}^0 p(x)\eta^-(x)\mathrm{d}x = \int_0^\infty p(-x)\eta^-(-x)\mathrm{d}x$. One can treat $\int_{-\infty}^0 p(x)\eta^-(x)\mathrm{d}x$ exactly as we treated $\int_0^\infty p(x)\eta^+(x)\mathrm{d}x$. The details are omitted for brevity.

References

[1] C. E. Shannon, *"Two-way communication channels"*, in Proc. 4th Berkeley Symp. Math. Statist. Probab., vol. 1, 1961, pp. 611-644.

[2] J. Schalkwijk, *"The binary multiplying channel–A coding scheme that operates beyond Shannon's inner bound region ,"* IEEE Transactions on Information Theory, 28:107-110, Jan 1982.

[3] J. Schalkwijk, *"On an extension of an achievable rate region for the binary multiplying channel ,"* IEEE Transactions on Information Theory, 29:445- 448, May 1983.

[4] J. Pieter, M. Schalkwijk,*"Extending The Achievable Rate Region Of The Binary Multiplying Channel,"* IEEE International Symposium on Information Theory, 1991 , pp.302, 24-28 Jun 1991.

[5] H.B. Meeuwissen, J.P.M. Schalkwijk, A.H.A. Bloemen, *"An extension of the achievable rate region of Schalkwijk's 1983 coding strategy for the binary multiplying channel,"* IEEE International Symposium on Information Theory, 1995, pp.445, 17-22 Sep 1995.

[6] T. S. Han, *"A general coding theorem for the two-way channel"*, IEEE Transaction on Information Theory, 30:35-44, Jan. 1984.

[7] Z. Zhang, T. Berger, and Schalkwijk, J. , *"New outer bounds to capacity regions of two-way channels,"* IEEE Transactions on Information Theory, vol.32, no.3, pp. 383-386, May 1986.

[8] J. Singh,O. Dabeer and U. Madhow, *"On the limits of communication with low-precision analog-to-digital conversion at the receiver,"* IEEE Transaction on Communications, vol. 57, pp. 3629-3639, December 2009.

[9] Y. Wu, L.M. Davis and R. Calderbank, *"On the capacity of the discrete-time channel with uniform output quantization,"* IEEE International Symposium on Information Theory(ISIT) 2009., pp.2194-2198, June 28 2009-July 3 2009.

[10] J. G. Smith, *The Information Capacity of Amplitude and Variance Constrained Scalar Gaussian Channels,* Inform. Contr., vol. 18, pp. 203-219, 1971.

[11] Su. Chandrasekaran, S. K. Mohammed, and A. Chockalingam, *"Achievable Rate Region of Gaussian Broadcast Channel with Finite Input Alphabet and Quantized Output",* Proc. NCC'2012, IIT, Kharagpur, February 2012

[12] S. Chandrasekaran, S. K. Mohammed, and A. Chockalingam, *"On the Capacity of Quantized Gaussian MAC Channels with Finite Input Alphabet",* Proc. IEEE ICC'2011, Kyoto, Japan, June 2011.

[13] B. Widrow, I. Kollar, *Quantization Noise*, Cambridge University Press, New York, 2008

[14] A. Sripad, D. Snyder,*"A necessary and sufficient condition for quantization errors to be uniform and white,"* IEEE Transactions on Acoustics, Speech and Signal Processing, vol.25, no.5, pp. 442- 448, Oct 1977.

[15] A. Tulino, S. Verdu, G. Caire and S. Shamai, *"The Gaussian Erasure Channel,"* IEEE International Symposium on Information Theory (ISIT), pp.1721-1725, 24-29 June 2007.

[16] W. Shuangqing, D.L. Goeckel and P.A. Kelly, *"Convergence of the Complex Envelope of Bandlimited OFDM Signals,"* IEEE Transactions on Information Theory, vol.56, no.10, pp.4893-4904, Oct. 2010.

[17] R. O'Neill, L.B. Lopes, *"Envelope variations and spectral splatter in clipped multicarrier signals,"* Sixth IEEE International Symposium on Personal, Indoor and Mobile Radio Communications, vol.1, no., pp.71-75, 27-29 Sep 1995.

[18] R. Gross, D. Veeneman, *"SNR and spectral properties for a clipped DMT ADSL signal,"* IEEE International Conference on Communications (ICC), vol.2, pp.843-847, 1-5 May 1994.

[19] H. Ochiai, H. Imai, "Performance analysis of deliberately clipped OFDM signals," IEEE Transactions on Communications, vol.50, no.1, pp.89-101, Jan 2002.

[20] L. Xiaodong Li, L.J. Cimini, *"Effects of clipping and filtering on the performance of OFDM,"* IEEE 47th Vehicular Technology Conference, vol.3, no., pp.1634-1638, 4-7 May 1997.

[21] L. Xia, T. Youxi, L. Shaoqian and L. Ying-tao, *"A minimum clipping power loss scheme for mitigating the clipping noise in OFDM,"* IEEE, Global Telecommunications Conference, vol.1, no. pp. 6- 9, 1-5 Dec. 2003.

[22] A. K. Khandani, *"Methods for spatial multiplexing of wireless two-way channels."* U.S. Patent 7 817 641, Oct. 19, 2010.

[23] T. Cover, A.E. Gamal, *"Capacity theorems for the relay channel,"* IEEE Transactions on Information Theory, vol.25, no.5, pp. 572- 584, Sep 1979.

[24] J. Harshan, B.S. Rajan, , "On Two-User Gaussian Multiple Access Channels With Finite Input Constellations," IEEE Transactions on Information Theory, vol. 57, no. 1299-1327, March 2011.

[25] L. J. Cimini , *"Performance studies for high-speed indoor wireless communications,"* Wireless Personal Communications, vol. 2, Issue 1-2, pp 67-85, 1995.